INTERUNIVERSITY PROGRAMME

MASTER OF SCIENCE IN WATER RESOURCES ENGINEERING

Vrije Universiteit Brussel
Katholieke Universiteit Leuven

Water quality monitoring of Schelde using in-situ, remote sensing technology and artificial neural network

By Zhiqi Wang

Promoter:
Prof. A. Van Griensven

Supervisors:
F. Khorashadi Zadeh
A. Baltodano Martinez
A. Nkwasa

Master dissertation in partial fulfilment of the requirements for the degree of

Master of Science in Water Resources Engineering

I

August 2022

Acknowledgments

I would like to express my deepest gratitude to my professor Ann, she is always full of passion, words cannot express my appreciation for her invaluable patience and expertise. I also could not have undertaken this journey without my supervisors Farkhondeh, Analy, and Albert, who generously provided knowledge and feedback. Additionally, thanks should also go to PARISlab@UCLA, a YouTube channel that made many great videos on ANN that educated and inspired me. Besides, I would be remiss in not mentioning my family, especially my mother, who gave me both spiritual and financial support. I am also grateful to my boyfriend Jacob, for his editing help and moral support. Their belief in me has kept my spirits high and continuously motivated me on this journey.

Finally, I want to thank myself for coming here. I was born in one of the thousands of small counties in China in 1997. When I was young, I lived an ordinary life with ordinary parents. I didn't know how rich the outside world is. I just wanted to study hard and get into a good university. After passing the college entrance examination, I came to Shanghai, the most prosperous city in China. Coming from a small county, college life was rich and colorful, my classmates interesting and diverse, and the city a place full of opportunities and distractions. While I was enjoying the high life of the city, I left behind nearly half of my high school classmates thousands of miles away in my hometown due to insufficient academic performance or family conditions, and I seemed to be burdened with their yearning for a better life.

After two years of university, I was fortunate enough to have the chance to study in Poland and to see the wider world. My family's income level deemed average in China would be considered poor by Belgian standards. Neither of my parents has ever attended university, but they still firmly believe that education can change one's destiny! For me to study abroad to obtain knowledge, they sometimes need to borrow money and were even prepared to sell their only real estate. Unlike many parents in my home country, they did not persuade me to stop my studies and start a family just because I am a girl but encouraged me to pursue higher education, find a suitable job that I like, and become self-reliant. Without any hesitation, I started my study abroad. When I first arrived in Europe, life was not as smooth as I imagined. Language barriers, dietary problems, racial discrimination, study pressure, difficulty in making friends, etc. hit me one by one. I was also plagued by depression for a long time. Fortunately, I met a group of very good friends and responsible and patient teachers who accompanied me through the storm before the rainbow. The moment I received my undergraduate diploma, the feeling I had was indescribable. I felt relaxed and grateful for the moment, as well as a yearning and worry for the future. Some of my friends of the same age are married and have children, and some have become rich by starting a business, especially the girls around me who have been urged by their parents to get married and return to work in China. It seems that continuing their studies is not the most "sensible" choice for a woman. I'm not the smartest among my female peers, and my learning ability is only average, under the prerequisite of fair competition, I don't think I deserve to achieve higher education. I can only thank the favor of fate, which let me be born into a family that has the conditions to choose the life I want. As I advance further in my studies, I feel like I carry with me the burden of the women whose opportunity for higher education had been forcefully taken away, and I hope to not let them down.

Abbreviations

ANN	Artificial neural network
RS	Remote sensing
AI	Artificial intelligence
Chl-a	Chlorophyll-a
SPM	Suspended matter
SST	Sea surface temperature
TSS	Total suspended solids
MODIS	Moderate Resolution Imaging Spectroradiometer
SeaWiFS	Sea-viewing Wide Field-of-view Sensor
MERIS	Medium Resolution Imaging Spectrometer
LEO	Low earth orbit
CMEMS	Copernicus Marine Service
RMSE	Root mean square error
MAE	Mean absolute error
PBAIS	Percentage Bias

Table of Contents

1. Introduction 10

2. Literature review 12

2.1 Application of remote sensing technology in water monitoring 12

2.2 Introduction of ANN model 13

2.3 Interested parameters 14

2.3.1 Chlorophyll-a 14

2.3.2 Turbidity 15

2.3.3 Water temperature 15

3. Material and methods 17

3.1 Experimental design 17

3.2 Study area 17

3.3 Data collection and scaling 19

3.3.1 Data collection 19

3.3.2 Data scaling 20

3.4 Modeling method 21

3.5 Statistical performance measures 23

3.5.1 Coefficient of determination (R^2) 23

3.5.2 Root mean square error (RMSE) 23

3.5.3 Mean absolute error (MAE) 24

3.5.4 Percentage Bias (PBIAS) 24

3.6 Build the ANN model 24

3.6.1 Pre-processing of model data 24

3.6.2 Build and run model 25

3.6.3 Model adjustment and visualization 25

4. Results 27

4.1 Comparison of in-situ data and RS measurement before modeling 27

4.1.1 The Correlation of RS and in-situ data before modeling 27

4.2 The ANN model performance visualization 31

4.3 The ANN model evaluation 33

5. Discussion 35

5.1 Station-wise accuracy of RS measurement 35

5.2 The performance of the ANN model 36

6. Conclusion & Recommendations 39
6.1 Conclusion 39
6.2 The future expectations 40
7. References 42

List of figures

Figure 1 - The Absorption Spectrum of both the chl-a and the Chl-b pigment (Gholizadeh et al., 2016) 15
Figure 2 - The map of the Schelde basin and the location of the measurement station 18
Figure 3 - Daily chlorophyll-a concentrations map of RS data 20
Figure 4 - Schematic of the ANN model input (remote sensing data) and output (in-situ data) 22
Figure 5 - ANN modeling flowchart use RS measurements and in-situ data 23
Figure 6 - Compare the RMSE of training set and validation set to find the desired neuron numbers for hidden layer 26
Figure 7 - Monthly average histogram for parameter a) Chl-a, b) Turbidity and c) Water Temperature 28
Figure 8 - The correlation plot of RS & In-situ data before modeling 29
Figure 9 - Correlation plot of RS & in-situ measurements of a) chlorophyll-a, b) SPM & turbidity and c) water temperature before modeling 30
Figure 10 - The regression plot of simulated RS data (ANN1 - with SPM, chl-a and water temperature as original input data) vs. the in-situ observation (target) 31
Figure 11 - The regression plot of simulated RS data (ANN1 - with estimated turbidity, chl-a and water temperature as original input data) vs. the in-situ observation (target) 32
Figure 12 - Visualize the prediction of the ANN model (ANN1 - with SPM as original RS data). 33
Figure 13 - Visualize the prediction of the ANN model (ANN2 - with estimated turbidity as original RS data) 33
Figure 14 - Histograms comparing ANN model performance by model evaluation parameters a) R^2, b) RMSE [ug/l] or [NTU] or [℃], c) MAE [ug/l] or [NTU] or [℃], and d) PBAIS (%) 34

List of tables

Table 1 - The information of the collected input and output data 21
Table 2 - Changes of prediction accuracy under different scenarios of ANN model 26
Table 3 - The most desirable model setting after the model adjustment 26
Table 4 - Training, validation, and testing regression results of the ANN models with different input combination 31
Table 5 - Comparison of the ANN model performance of the water quality parameters 34
Table 6 - Pearson's correlation coefficient (R) between in-situ data and RS data and ANN prediction RS data 35

Abstract

Water quality is usually assessed using physical, chemical, and biological parameters. However, traditional field observations are difficult to be useful at larger temporal and spatial scales because they are too time-consuming and expensive. The use of remote sensing (RS) techniques in water monitoring and management has long been recognized as they can repeatedly monitor large areas in a short time and reduce the cost and labor required for measurements. Besides, in response to the increasing complexity of water quality models, traditional numerical models have been difficult to meet the needs of solving some specific problems. The use of artificial intelligence (AI) techniques combined with these mathematical models is widely used by an increasing number of researchers. Within this, the artificial neural network (ANN) approach is known as a powerful tool for modeling many nonlinear hydrological processes and solving complex problems. It has the advantage of representing complex nonlinear relationships between the inputs and outputs without any mathematical algorithms, and learning these relationships directly from the modeled data, which makes modeling faster and more flexible.

This study tried to combine the powerful observational capabilities of remote sensing (RS) technology in time and space with the modeling flexibility of artificial neural networks (ANN) to provide a practical solution for river water quality assessment. The results of the study approved that the feedforward ANN model can well predict the water quality parameters such as chlorophyll-a concentration, turbidity, and water temperature in the estuary from satellite data, it's fitting ability with in-situ data has significantly improved compared to the original remote sensing data, showing its potential in water quality modeling. In addition, the difference in the input dataset (RS products) in the model could lead to markedly different simulation results, the more accurate the input dataset is, the higher the model performance. This also confirms that artificial neural networks as a data-driven model, the quality of data in the input model can play a decisive role in the model performance.

Keywords: *remote sensing; water quality; rivers; estuary; artificial neural network*

1. Introduction

Due to overpopulation and waste(water) discharge that exceeds the natural endurance, the global freshwater system is facing resource shortages and water pollution problems There is an urgent need for more effective and sustainable freshwater resource management. As an important part of freshwater resources, rivers are also facing problems such as water quality decline, eutrophication, and ecological degradation. The sharply rising water level during heavy rains could easily cause damage to the ecology and the social economy. It is known that rivers play an important role in ensuring the safety of drinking water and the ecology of the watershed, it has a significant impact on the economic and social development of the watershed as well. Among them, estuary monitoring occupies a very important and special position.

Estuaries are typically biodiverse areas, as the interface between terrestrial and coastal waters, they not only have complex dynamics but also support many biochemical processes that are critical to global ecology through the high yields of biological communities, this ecological function with great potential makes the estuary occupy an irreplaceable position in controlling the water quality of coastal waters (Damme et al., 2005). Around the estuary, there are always many urban or agricultural areas, which lead it usually served as the downstream recipient of sediments or land discharges (Hu et al., 2004). With the increase of anthropogenic activities in recent years, the estuary ecology is also under greater pressure. Therefore, the establishment of continuous monitoring and evaluation of the impact of these natural or anthropogenic pressures on the estuary and local ecology is of great significance. Effective, stable, and long-term applicable monitoring tools are a must.

As a tool for water quality assessment, in-situ measurement is accurate in time and space, but it is difficult to express the spatial or temporal view on a larger scale (AL-Fahdawi et al., 2015), besides, traditional in-situ measurement is usually time-consuming and costly. Due to these limitations, it is expected to develop and utilize tools more suitable for long-term large-scale water quality monitoring. The application of RS in water monitoring and management has long been recognized, RS not only can be used to monitor water quality parameters (i.e. turbidity, chlorophyll, and temperature) but can also expand field observations, reduce the cost and labor requirements of data measurement (Ceyhun & Yalçın, 2010).

In Europe, various regulations have established requirements for comprehensive water quality monitoring to assess the ecology of coastal waters, including the European Union's Water Framework Directive (*Water Framework Directive*, n.d.) and the Marine Strategy Framework Directive (Marine Strategy Framework Directive), 2008). These regulations impose stricter requirements in anticipation of promoting and making full use of advanced methods such as automated monitoring (Attila et al., 2018). It makes the data based on traditional monitoring sites can hardly meet the current state assessment requirements of water bodies. However, while the ability of RS to assess water quality cannot be underestimated, the technology itself is not precise enough, and more accurate data must be used in conjunction with traditional sampling methods and field measurements (Gholizadeh et al., 2016).

For ecosystem monitoring and management, accurate and reliable predictions are critical. Researchers say that the limitations of water quality data and the high cost of water quality monitoring often make analytical modeling very difficult (Hameed et al., 2017a) and that traditional methods of water quality analysis involve lengthy calculations and consume a lot of time. Therefore, artificial intelligence (AI) offers the

best solution because it is not only very efficient in terms of computational speed, but also requires much fewer input parameters and input conditions than deterministic models. In recent years, AI such as ANN have been successfully used in various water engineering related cases. ANN technology has also begun to be widely used in model optimization, data prediction and so on in the field of water resources (Hameed et al., 2017b). ANN technology can deal with unknown knowledge, it can not only represent a complex nonlinear relationship between the input and output of any system but also learn these relationships directly from the data being modeled. Most studies have shown that neural networks have better predictive power than traditional models because they can flexibly represent relationships between different systems (Chang & Liao, 2012).

In the selection of parameters for monitoring water quality changes, identifying some parameters that are relatively easy to collect and directly related to ecosystem stress can help provide a very good basis for modeling. Evidence of changes in estuarine ecological characteristics are known to include increased phytoplankton abundance, decreased water clarity (Hu et al., 2004). Then parameters such as chlorophyll-a (chl-a), suspended sediment concentration (turbidity), water temperature, salinity, and oxygen demand are relatively appropriate water quality parameters. In addition, since RS technologies mostly use satellites and drones, and most aquatic ecosystems are a mixture of optical shallow water and optical deep water (Palani et al., 2008), the complexity of this type of optics is very important for water quality monitoring applications. After comprehensive consideration, several parameters that are easier to be monitored by RS and stable for long-term data recording are finally selected as the water quality parameters in this study, which are chlorophyll a, turbidity, and water temperature. Among them, the chlorophyll-a and turbidity can reflect the degree of eutrophication of the water body, turbidity describes the clarity of water, which varies with seasonal or external discharges, and changes in water temperature affect cyanobacterial growth rates and biogeochemical processes, it also has influences on other parameters.

In recent years, many studies have confirmed that ANN techniques are known to have excessive potential in the field of water engineering, but there are few cases where ANN has been applied to estuarine water quality prediction, so this study aims to apply it to in-situ measurements and satellite imaging at an estuary in Belgium to analyze the local estuarine water quality. The aim is to evaluate the performance of the combined use of remote sensing and ANN to monitor water quality variables (temperature, turbidity, chlorophyll-a) in the Scheldt estuary.

This study discusses the use of RS for monitoring estuarine water quality parameters and compares the results with field measurements. An ANN model will be trained and optimized so that the input satellite data can be used to predict as closely as possible the in-situ measurements. The model can be used to monitor and predict changes in river water quality more consistently and effectively. The ideal result of the study is that the trained ANN model can provide ideal simulation values for the research target, and reveal the potential of the ANN model in simulating water quality variables, which could be used to provide water quality early warning information to help managers improve lake ecology efficiency of protection (Palani et al., 2008).

2. Literature review

2.1 Application of remote sensing technology in water monitoring

Remote sensing (RS) water quality products were originally developed for global ocean observations, dating back to the early 1970s when airborne and satellite sensors were used to examine a wide range of water quality constituents (Topp et al., 2020), the development of satellite technology has allowed measurements to be made on a global scale, although the local resolution is generally poor (Keith et al., 2014). RS methods for water monitoring have been available since the early 1980s, however, at this time RS techniques relied on the ability to measure changes in spectral features backscattered from water, correlating the measured changes with water quality parameters through numerical models (Ritchie et al., 2003). It was only in the last two decades that the further development of space-based tools led to a shift in focus in the field from a focus on method development to a greater focus on water quality dynamics, with RS techniques being applied more often to assess the environment in the ocean and adjacent land areas (Hu et al., 2004). Much of this shift has been caused in part by the development of satellite technology and in situ measurement techniques, as well as increased computing power. Emerging resources such as improved data availability and enhanced processing platforms have helped researchers to address challenging scientific questions (Topp et al., 2020).

RS allows not only data collection but also data analysis using satellite multi-(hyper)spectral sensors, UAVs (Unmanned aerial vehicles), or aircraft, allowing meaningful spatial information to be extracted from remotely sensed data. Compared to traditional data collection and analysis methods, this technology allows a wide range of RS images to be acquired on a spatial and temporal scale, providing users with low-cost and efficient spatial information. However, the quality of the information depends on weather conditions and calibration for the type of site being observed (lake, river, groundwater, etc.). Among the various terrestrial RS systems, 75% of studies have focused on lakes and water quality parameters associated with lakes (Topp et al., 2020). Among these, measurements of eutrophication-related parameters occur almost exclusively in lake systems, such as chlorophyll, turbidity, etc. Eutrophication in rivers and estuaries has been relatively very little studied, mostly interested only in sediment load, total suspended solid (TSS), etc. The ocean RS system, on the other hand, performs better with its many ocean color sensors with higher spectral resolution and frequent return cycles, including MODIS (Moderate Resolution Imaging Spectroradiometer), SeaWiFS (Sea-viewing Wide Field-of-view Sensor) and MERIS (Medium Resolution Imaging Spectrometer), which are developing faster in water quality analysis applications are also very diverse. However, their disadvantage is the lack of higher spatial resolution to observe narrower inland water bodies, such as rivers.

The continuous global data record from the low earth orbit ocean color satellites has been 20 years, and it is subordinate to a variety of instruments performing the task of collecting RS data, including SeaWiFS, MODIS, and the WQAS (Water Quality Analysis System) that from NASA, and the sensor MERIS which from ESA (Werdell et al., 2018). However, regardless of the sensor, controlling for different atmospheric influences is one of the biggest obstacles for RS of waters, as atmospheric conditions can vary very significantly and therefore water quality parameters can only be estimated accurately with accurate atmospheric corrections. In recent years, improvements in atmospheric correction algorithms for complex waters have been achieved by using

algorithms such as radiative transfer functions and dark pixel extraction to analyze chlorophyll, and suspended sediments, which usually involve multiple computationally expensive functions (Topp et al., 2020). As computer performance continues to improve and more research introduces advanced machine learning methods such as ANN, the global applicability of ANN-based algorithm development, such models have gradually started to be used routinely, thus helping to produce more robust RS integration results.

2.2 Introduction of ANN model

McCulloch and Pitts (1943) are the researchers who first introduced the concept of artificial neurons, after them, the development of ANNs has gained acceleration. Due to the development of more sophisticated training algorithms at the end of the last century, the major applications of ANNs in solving complex problems have become popular (Altunkaynak, 2007). The ASCE Task Committee on Application of ANN in Hydrology (Govindaraju, 2000) has published research on the role of ANNs in hydrology, and concluded that ANNs are robust tools for modeling many nonlinear hydrological processes, such as rainfall-runoff, water quality modeling, precipitation, etc.

Traditionally, numerical models have often been used to simulate coastal ecosystems and processes of change, and appropriate algorithmic procedures have been used to solve specific problems. However, due to the complexity of numerical simulations of water quality, there is a growing need to combine increasingly sophisticated AI techniques with these mathematical models to streamline operations and make predictions more accurate. In the direction of water quality simulation, there are a variety of technologies contributing to AI, including knowledge-based systems, genetic algorithms, ANN, and fuzzy inference systems. These technologies contribute to models in more than just different areas and may not be mutually exclusive. Among them, ANN, as an evolving technique, has been widely used for its ability to cope with uncertainty in complex situations, as a data-driven modeling approach, it has been used in water quality modeling for many years (Chau & Cheng, 2002).

An ANN model can be regarded as a "black box" model, which can not only represent a complex nonlinear relationship between the input and output of any system, but also learn these relationships directly from the data being modeled (Chang & Liao, 2012). In water environment science, ANN modeling can be applied to rainwater, water level prediction, etc. Through continuous adjustment of parameters, the simulated value can be finally made similar to the measured value (Chang & Liao, 2012), it has better predictive power than conventional models. A classic ANN model uses a typical three-layer feedforward architecture, including an input layer, a hidden layer, and an output layer, these layers are composed of many simple processors. Learning is getting the computer to find a valid setting for all the weights and biases so that it will solve the problem. The data is divided into three sets: a training set, a validation set, and a test set, perform model training and testing by adjusting the number and combination of hidden layer neurons to determine the optimal number of hidden layer neurons (Wang et al., 2013). The main statistical tools of the model are the root mean square error (RMSE) and the coefficient of determination (R^2), RMSE which is a statistical measure of the difference between the actual output and the output predicted by the network model, the R^2 can be used to explain how much variability is caused between two factors. As Recknagel (1997) mentioned that ANNs can achieve high R^2 values, especially for total cyanobacterial populations, but there is no clear description of the actual process. The advantage of this model is that it does not require any mathematical

algorithms, and the modeling method is faster and more flexible. In addition, its nonlinear relationship modeling ability is very suitable for water quality modeling and prediction and has a high fault tolerance (Zhang & Stanley, 1997).

However, it appears that most studies have been based on lake systems or river systems, and relatively few studies have been conducted on neural network modeling of estuarine systems. In addition, the reference variables of the ANN model in many studies do not consider the optimal choice of the current environment, but only all possible environmental parameters in the model, and because of the "black box" structure is also difficult to extract the experience and laws from the model, so the technology in the simulation and prediction of water quality there is much room for improvement. This study takes advantage of the modeling flexibility of ANNs and combines them with RS images, allowing it to use image values directly in estimation without refining other environmental factors, greatly improving the efficiency of the analysis.

2.3 Interested parameters

Water quality research is the process of determining the chemical, physical and biological characteristics of a water body and identifying the sources of water pollution and its minimization. According to the suggestion from House (1989) suggested that in order to select a variable, three criteria need to be met: (a) data of the variable are readily available; (b) it should be a significant indicator of water quality change or pollution; (c) the maximum water quality criteria should be set for the selected variable. RS technology has enhanced the scope of water quality monitoring by providing a spatial and temporal view of surface water quality parameters, making it possible to monitor water bodies more effectively and quantify water quality problems. Known commonly used parameters to measure water quality are chlorophyll-a, water temperature, oxygen demand, total organic carbon, total phosphorus, total nitrogen, etc. However, when we refer to RS technology to observe water quality because most of its research is focused on optical activity variables, some parameters because of their weak optical properties are less likely to be applied to RS monitoring, while parameters such as chlorophyll a, total suspended solids (TSS) and turbidity can be more accurately expressed (Gholizadeh et al., 2016). After repeated measurements, the following three parameters became the most interesting estuarine water quality parameters for this study.

2.3.1 Chlorophyll-a

Chlorophyll-a (chl-a) is one of the most important indicators to define the eutrophication of a water body, and it has a significant correlation with the nutrient content in the water and water quality (Schaeffer et al., 2012). Chlorophyll-a is used in oxygenated photosynthesis and is present in plants, algae, and cyanobacteria. Chlorophyll-a, which reflects mainly green in the spectrum, also absorbs energy from violet-blue and orange-red wavelengths. Figure 1 shows the absorption spectra of chl-a and chl-b. A review of the literature indicates that a large number of studies have focused on RS measurements of chl-a concentrations, and most algorithms for determining chl-a concentrations require a wavelength close to 675 nm and another close to 700 nm (Gholizadeh et al., 2016).

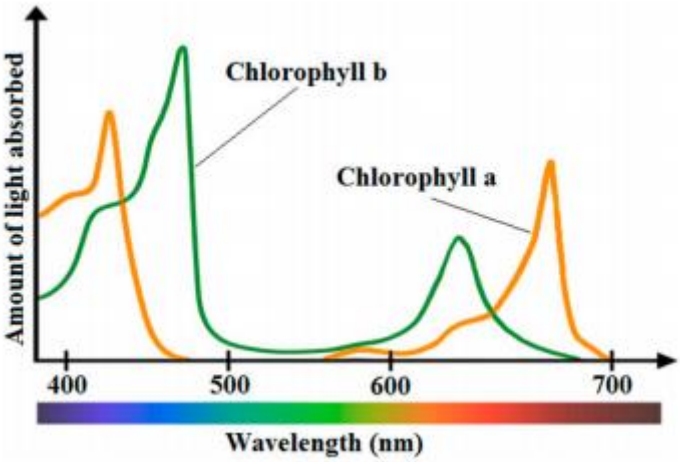

Figure 1 - The Absorption Spectrum of both the Chl-a and the Chl-b pigment (Gholizadeh et al., 2016)

By referring to the research of (Wang et al., 2013), and Salman et al. (2013), it is determined that the chlorophyll-a concentration will be one of the water quality parameters in this study. The challenge of this research is the optical complexity of inland waters. The optical absorption and scattering of lake waters will cause optical variability, which makes water quality monitoring using RS data more difficult (Wang et al., 2013).

2.3.2 Turbidity

Turbidity, which indicates the transparency of water, is an optical characteristic of water quality. It not only reflects the concentration of suspended matter in water but is also the most direct evaluation of water quality by the human senses. Turbidity is a measure of the light scattering properties of water, where the complex nature of the suspended matter in water alters the reflectance of the water, resulting in a change in color. Turbidity and total suspended matter (TSPM) are considered important variables in many studies because their association with incoming sunlight in turn affects photosynthesis for algal and planktonic growth (Chang & Liao, 2012).

RS techniques are widely used to estimate and map the turbidity and concentration of suspended particles and to provide their spatial and temporal variability. There is a significant relationship between turbidity and suspended sediments and the radiance or reflectance in spectral (Chebud et al., 2012). An in-situ study by Ritchie (2003), showed that spectra in the range of 700-800 nm were most useful in determining suspended particles in the water column.

A review of the literature suggests that MODIS is one of the most often used sensors to obtain the SPM data or the turbidity estimated from SPM products. Neural network models are also often used to interpret images and to evaluate the turbidity of simple linear regression methods. It is important to note in the modeling process that more care should be taken in the selection of the transfer function and the number of neurons in the hidden layer since water turbidity is less sensitive to training time and learning speed.

2.3.3 Water temperature

Water temperature is the main model predictor (31.5% of publications) (Rousso et al., 2020a) for water quality. Higher water temperature generally speeds up the growth rates of cyanobacteria and biogeochemical processes. Temperature regulators physical,

chemical, and biological processes in water, which can be used to estimate the primary production and growth rate of phytoplankton. Besides, the distribution, transport, and interaction of some nutrients have a significant relationship with the temperature of the water body (Gholizadeh et al., 2016) It also presents obvious seasonal changes as well. In addition to its own effects, it also influences other parameters and can alter the water's physicochemical properties.

Since temperature is stratified within the body of water when observed using RS techniques, remote sensing-derived temperature estimates must be evaluated with great care in situations such as after rainfall. Fine pixel-sized measurements of river temperature are useful for studying fine-scale spatial variations and patterns of river temperature in relation to hydrological features such as groundwater input. Emission of infrared radiation (3-14μm) is a well-established practice, especially in oceanography, where daily observations of regional and global sea surface temperature (SST) using satellites are common. The SST accuracy of the infrared radiometer is around 0.5℃, but its use in shady areas is limited due to the presence of weather factors such as clouds or fog (Gholizadeh et al., 2016).

3. Material and methods

3.1 Experimental design

This study proposes a remote sensing-based method and develops an ANN model to quantify the water quality parameters of the target river. In addition, the study will be based on many simulations in MATLAB software to achieve this model and evaluate the fit and stability of the model. The aim is to rely on the training and optimization of the model so that the input RS data can be simulated as close as possible to the in-situ measurements.

As for the training of the ANN model, it was using a typical three-layer feedforward architecture, which includes an input layer, hidden layer, and output layer. the RS data will be the input of the ANN model, and in-situ data with be the output. The current simulating parameters are chlorophyll-a, turbidity, and water temperature.

To verify the performance of the trained ANN, one study measured point in the estuary of Schelde river was introduced as the study case. The RS time series data was generated from a selected pixel at the mouth of the estuary and used the data from a monitoring station close to the river mouth for comparison. The ideal result is that the trained ANN model can provide stable and accurate simulation results for the desired targets (Palani et al., 2008).

3.2 Study area

The catchment area of the Schelde is 20331 km^2, and about 10.4 million people are living In this region, which has a very dense population that could count up to over 500 inhabitants per km^2 (Billen et al., 2005). The Schelde estuary is in Northern Belgium (Flanders) and the Southwest Netherlands (Figure 2). It extends from the mouth at Vlissingen (0 km) till Gent (158 km). Near the Dutch and Belgian border, the estuary narrows and becomes characterized by a single tidal channel and is called Sea Schelde (Zeeshcelde in Dutch). The Sea Schelde consists of two parts, one part is stretching from Antwerp to the upstream boundary at Gent, called Upper Sea Schelde (Boven-Zeeschelde in Dutch), and another part is the Lower Sea Schelde (Beneden-zeeshelde in Dutch), which stretches from the Dutch Belgian border to Antwerp (Damme et al., 2005). The study point of this study is in the Lower Sea Scheldt (Beneden-zeeshelde in Dutch), all the studied the in-situ time-series data was provided by the station Liefkenshoek (Figure 2). Within the selected water quality parameters, chlorophyll-a concentration is thought to be controlled largely by sediment resuspension and local annual precipitation, turbidity is of great interest in estuary due to light-attenuating effects as well, especially the nutrient input, and sediment transport and deposition into shipping channels (Hu et al., 2004).

In the past several decades, the Schelde basin experienced an extreme case of water pollution due to its intensive human activities here, such as active industrial development, agriculture, and farming activities. As a link between the land and the sea, the ecosystem of the Schelde estuary is under constant pressure from human activities. The concentrated large industry and the intensive agriculture in the catchment area lead to excessive nutrient inputs to the estuary, which is considered one of the main contributors to the decline of river water quality part (W. Baeyens et al., 1998). Even though the local government has invested a lot in the improvement of water quality, and the results are beginning to bear fruit, such as undertaken industrial and municipal

wastewater treatment since the 90s in Flanders, however, untreated municipal wastewater is still being discharged into the estuary till today (Billen et al., 2005), therefore, continuous monitoring and improvement of local water quality are still necessary.

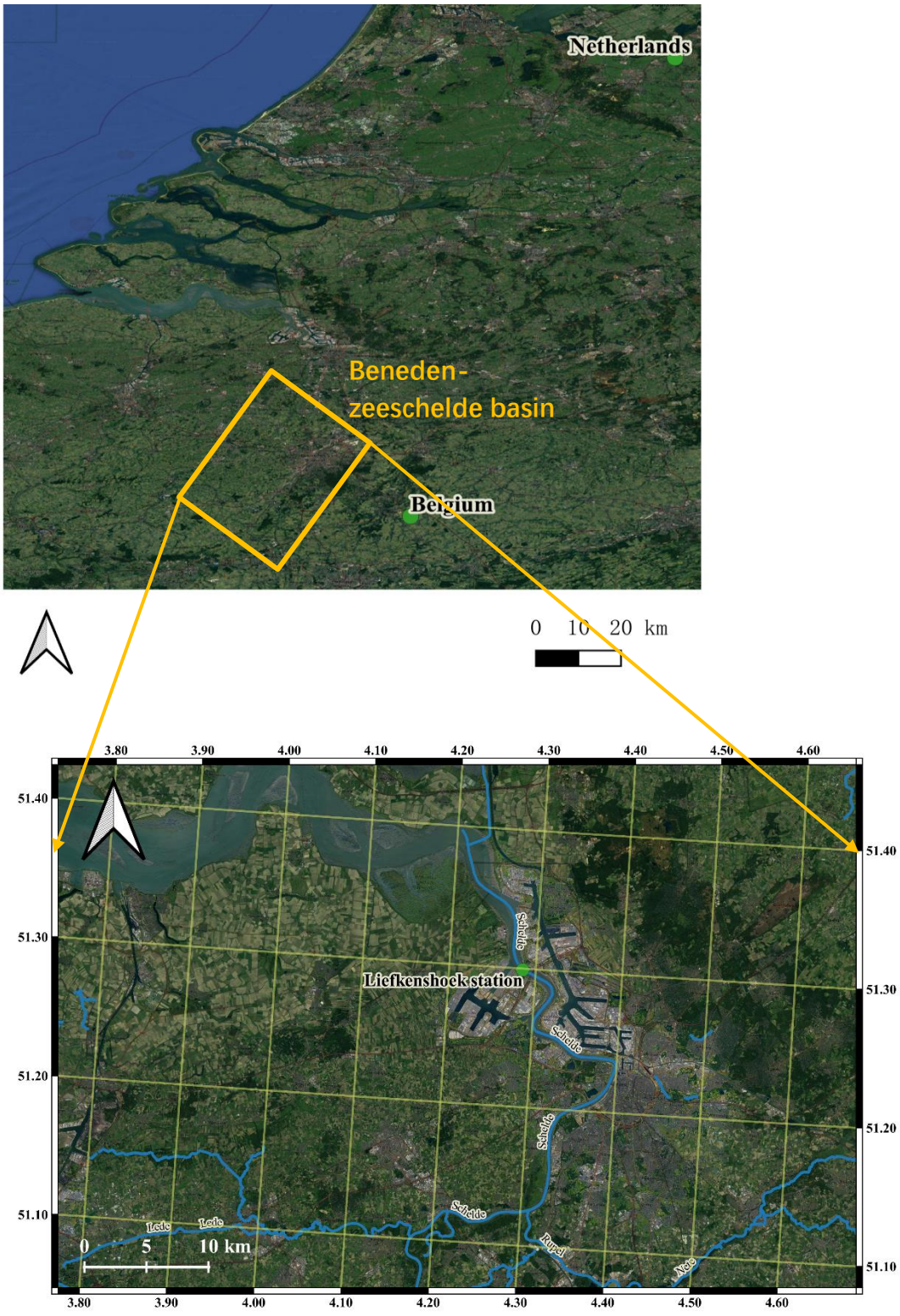

Figure 2 - The map of the Schelde basin and the location of the measurement station

3.3 Data collection and scaling

To process the data for this model, first, collect time series data for the input and output parameters of the model. After evaluation of the practical conditions, the satellite data is chosen as the input parameters of the ANN model, and in-situ measurements dada will use as output targets. The main purpose of known source data analysis is to pick an appropriate architecture for the neural network model. The in-situ measurement data comes from the meteorology station near the Schelde estuary, the chosen output in this model is parameters include chlorophyll-a, turbidity, and water temperature. The satellite data in this study comes from the Global Ocean Satellite Observations project which was developed by The Copernicus Marine Service (CMEMS). The chosen input satellite parameters include chlorophyll-a, suspended matter (SPM), and water temperature, all the RS data were downloaded from the coordinates most close to the meteorology station (Figure 2) to keep the input and output data as close and relevant as possible.

3.3.1 Data collection

The Liefkenshoek station is the only meteorology station selected for the study within the estuary. Because this station provides chlorophyll-a, turbidity, and water temperature with 5min interval from June 2019 to the present. This might help maintain consistency when analyzing and scaling data. All the in-situ time series data was downloaded from the "WaterInfo" website (https://www.waterinfo.be) and then converted into weekly average data. "WaterInfo" is a website of the Flemish government with open access to the public. It provides accurate and on-time water information in Belgium. It includes many measurements and forecasts of the water, floods, and droughts (*Waterinfo*, n.d.).

During this study, the satellite data of water temperature is from the Ocean Physical-Wave Analysis and Forecast Product, which is supported by The Copernicus Marine Service (CMEMS). These products are generated by a coupled physical-wave forecasting system for European at 1.5 km horizontal resolution, the measured variables include surface temperature, salinity, horizontal currents, sea level, etc. (*NASA Ocean Color*, n.d.).

The satellite data of chlorophyll-a and Suspended Matter (SPM) are from the Ocean Colour products (*GlobColour*, n.d.) with the supporter from Copernicus Marine Service (CMEMS), which is presently supported by the Copernicus-GlobColour processor. The products include chlorophyll-a (1km resolution in Europe), Suspended Matter (SPM) with 4 km spatial resolution, and other optical products. About the characteristics of the products, time coverage is from 1997 to the present, time resolution includes daily, weekly, and monthly. The sensors for the products are based on the merging of the sensors SeaWiFS, MODIS, etc. This project is a new empirical algorithm for retrieving chlorophyll using data collected primarily by SeaWiFS and MODIS (Aqua). This algorithm is for estimating surface chlorophyll concentrations from satellite ocean color measurements, it shows superior in reducing the chlorophyll ≤ 0.25 mg/m^{-3} uncertainty to existing algorithms. A commonly used field-of-view sensor (SeaWiFS) is a satellite-based sensor designed to provide quantitative data on the optical properties of global ocean life, specifically for monitoring ocean features such as chlorophyll-a concentration and water clarity (*SeaWiFS*, n.d.). The Moderate Resolution Imaging Spectroradiometer (MODIS-Aqua) instrument collects data across the Earth's surface,

which aims to improve our understanding of global dynamics and processes on land, oceans, and the lower atmosphere (NASA Ocean Biology Processing Group, 2017).

3.3.2 Data scaling

For in-situ data, first, obtained the 5-min time series data for all three products from the meteorology station, which is from April 2019 to March 2022. Then eliminated data of poor monitoring quality and extreme data, and the missing data were filled using the interpolation method (i.e., Kriging). Next, convert the obtained data to weekly time-series data, this step is very crucial because firstly this study is mainly looking at seasonal changes, very detailed data are not needed, and secondly, it helps to avoid missing data.

For RS data, to process the data scaling, first imported the RS products to python to view the satellite image. Due to different RS products giving different resolutions of the images, so the next step was to interpolate all products to have the same coordinates and resolution (1 km X 1 km). It is aimed to minimize the differences between different products in geography, reduce the occurrence of errors, and make the values obtained more relevant. After the Lienfkenshoek station coordinate (latitude 51.3, longitude 4.3) was located in the satellite image, or the nearest coordinates to the station were located (Figure 3), all the time series data from April 2019 to March 2022 was extracted from this coordinate. Due to the datasets were not very complete, all the daily data was converted to the average weekly data like in-situ data to make a compromise.

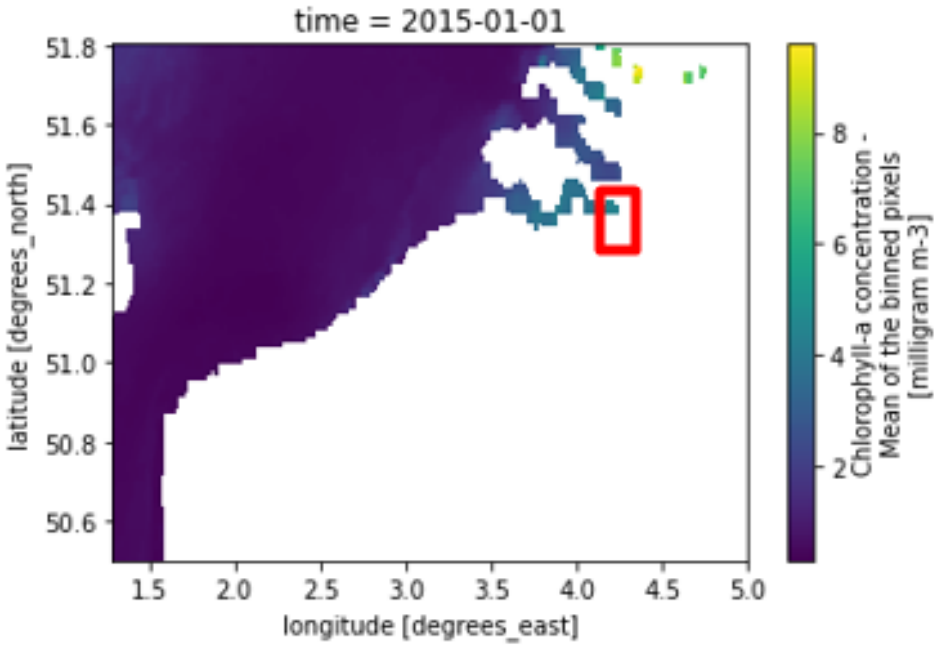

Figure 3 - Daily chlorophyll-a concentrations map of RS data

Another detail worth noting is that for the input data (RS data), the SPM parameter was used instead of the turbidity to be the same as the output parameters (in-situ data). As the RS products of turbidity in coastal waters are less numerous than those of SPM, therefore, this study employed the estimation of turbidity using a mathematical method proposed by Nechad et al. (2009). In this mathematical method, chlorophyll concentration and non-algal SPM are two variables used for the validation of the ecological model. Thus, the turbidity was expressed by the combination of these two variables:

$$\text{Turbidity} = \alpha\,(\text{SPM} + 0.234 * \text{Chl}^{0.57}) \quad (1)$$

The term α in Eq. (1) is obtained by regression of turbidity on SPM at the Liefkenshoek stations, the value of α was determined to be 1.19. The term 0.234 *$\text{Chl}^{0.57}$ represents the biomass of phytoplankton which is related to the chl-a concentration (Gohin, 2011).

Based on this, this study compared the fitting results of two models, one that directly applied SPM data as one of the inputs, and the other that applied estimated turbidity as the input instead of SPM to the model. The table below lists information on the collected RS and in situ data (Table 1).

Table 1 - The information of the collected input and output data

Raw Data	***Coordinates***	***Parameters***	***Data***	***Resolution***
Input - *Remote sensing*	Latitude 51.38, longitude 4.234	Chlorophyll-a	Daily (Converted to weekly)	1 km X 1 km
		SPM	Daily (Converted to weekly)	4 km X4 km (Interpolated to 1km)
	Latitude 51.35, longitude 4.24	Water Temperature	Daily (Converted to weekly)	1.5 km X 1.5 km (Interpolated to 1km)
Output - *Station Liefkenshoek*	Latitude 51.3, longitude 4.3	Chlorophyll-a	5 min (Converted to weekly)	-
		Turbidity	5 min (Converted to weekly)	-
		Water Temperature	5 min (Converted to weekly)	-

3.4 Modeling method

The training of the model is completed by constructing input-output mapping. This study uses a typical three-layer feedforward architecture, which are the input layer, hidden layer, and output layer. For the hidden layer, there can be one or more hidden layers in the middle to express the complex associations between the networks. All hidden and output neurons are processed by employing a nonlinear transfer function to produce results, and after many experiments to determine the neurons within the hidden layer's optimal quantity (Chau & Cheng, 2002). As shown in Figure 4, the input layer of this ANN model consists of three neurons, which are the three parameters from satellite data. The parameters included chlorophyll-a, suspended matter (SPM) or estimated turbidity, and water temperature. While the three in-situ measured parameters are the corresponding model's output neurons, including chlorophyll-a, turbidity, and water temperature.

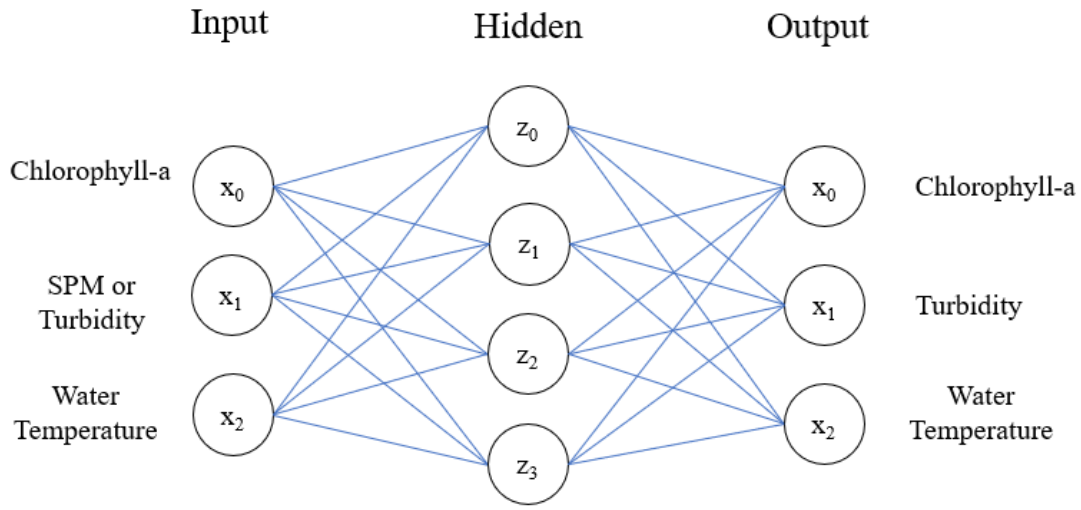

Figure 4 - Schematic of the ANN model input (remote sensing data) and output (in-situ data)

The modeling process was divided into four stages: source data collection and analysis, neural network construction and startup, model adjustment, and model evaluation, the detailed shown in the modeling flowchart (Figure 5).

In the first stage, in-situ data were collected from one meteorology station and the satellite data with corresponding parameters were collected. Afterward, these datasets were visualization in python and undergo fining and normalization. The second stage is the initiation of the model. The structure and parameters of the model were determined by the ANNs model proposed in Figure 4, the model was created as a shallow network with one hidden layer. It is worth to emphasize that the setting of neurons number in this layer is crucial, and the model parameters can be adjusted through training and testing. In the third stage, the collected data was split into the training set, the validation set, and the testing set. When dividing the data, the size is 50%, 20%, and 30% separately. First, imported the training set into the model to train the model to optimize the parameters of the model, which are the weights of the connection between the neurons and the value of the bias. Then, used the validation set to optimize the internal parameters to obtain the desired results. This can be done through the adjustment of the number of neurons and the number of the hidden layer, aiming to minimize the error. The last stage is model evaluation. After obtaining the optimized model, imported the testing set of RS data into the optimized model to get the simulated result. Then, the simulated results were compared with the in-situ data to evaluate the accuracy and stability of this model. The purpose of model evaluation is to evaluate the ability of ANN to recognize the patterns presented in the training data set and reproduce them.

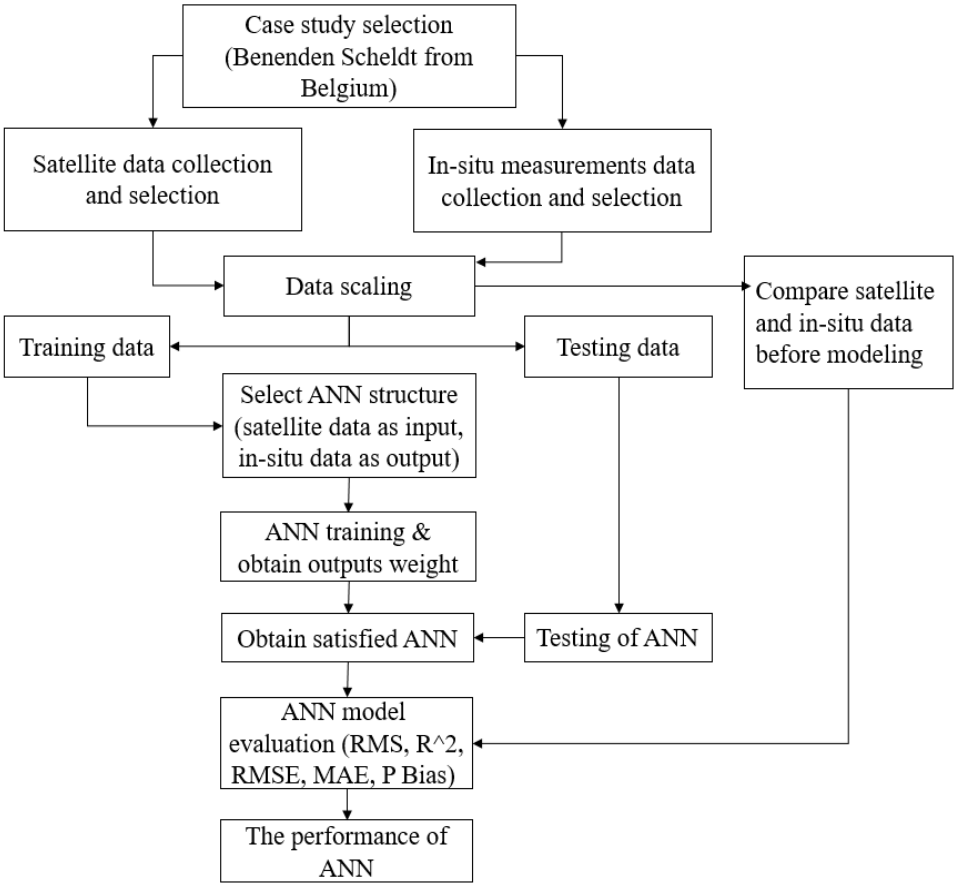

Figure 5 - ANN modeling flowchart use RS measurements and in-situ data

3.5 Statistical performance measures

The selected measures to evaluate the performance of the model are four quantitative statistical indicators: coefficient of determination (R^2), root mean square error (RMSE), mean absolute error (MAE), and Percentage Bias (PBIAS).

3.5.1 Coefficient of determination (R^2)

The coefficient of determination (R^2) is the square of the correlation coefficient (R). The R^2 shows the degree of the linear relationship between observed and simulated data, and can be used to explain how much variability is caused by two factors (D. N. Moriasi et al., 2007). Its value ranges from 0 to 1, the closer the value is to 1, the better the fit or relationship between the two factors, typically values greater than 0.5 are considered acceptable. R^2 is calculated as shown in Equation (2):

$$R = \frac{\sum_{i=1}^{N}(x_i - \bar{x})(y_i - \bar{y})}{\sqrt{\sum_{i=1}^{N}(x_i - \bar{x})^2 \sum_{i=1}^{N}(y_i - \bar{y})^2}} \quad (2)$$

3.5.2 Root mean square error (RMSE)

RMSE describes the size of the average error between the observed value and the model result. The RMSE is an evaluation of the difference between the actual output value and the output value predicted by the model while the threshold minimum square error value or the square error of the test set is reached, training stops when RMSE is rising. Due to calculation time considerations, as long as the number of good patterns

is greater than 98%, the training process can usually be stopped (Kisi, 2013). The equation of RMSE is shown in Equation (3):

$$RMSE = \sqrt{\frac{\sum_{i=1}^{N}(y_i - x_i)^2}{N}} \quad (3)$$

3.5.3 Mean absolute error (MAE)

MAE, like RMSE, is an error index widely used in model evaluation, it indicates the error in units (or square units) of the component of interest (D. N. Moriasi et al., 2007), which helps in analyzing the results. In general, half the standard deviation of the measurement data can be considered low. MAE represents the average value of the absolute error between the predicted value and the observed value, it is a linear score, and all individual differences have the same weight on the average value. The equation of MAE is shown in Equation 4:

$$MAE = \frac{\sum_{i=1}^{n} abs(y_i - x_i)}{n} \quad (4)$$

3.5.4 Percentage Bias (PBIAS)

Percent bias (PBIAS) measures the deviation of the simulated data from their observed counterparts, it is expressed as a percentage. The lower the PBIAS value, the more accurate the model simulation. Positive values indicate model underestimation bias and verse vise (Gupta et al., 1999). In general, model simulation can be judged as satisfactory if PBIAS ± 25% for streamflow (D. N. Moriasi et al., 2007). The reason for selecting the PBIAS index is it can clearly indicate poor model performance. Especially during watershed simulation, PBIAS values for streamflow tend to be more variable during dry years than during wet years among different autocalibration methods (Gupta et al., 1999). PBIAS is calculated with Equation 5:

$$PBias = \left[\frac{\sum_{i=1}^{n}(x_i - y_i) * (100)}{\sum_{i=1}^{n}(x_i)}\right] \quad (5)$$

Among them, x_i is the observation value, y_i is the satellite simulation value, n is the number of time steps, $\bar{x}$ is the mean value of the observation data, and $\bar{y}$ is the is mean value of the satellite simulation output (Kisi, 2013).

3.6 Build the ANN model

3.6.1 Pre-processing of model data

First, as mentioned previously, the purpose of this study is to rely on the training of the ANN model, so that the input remote sensing (RS) data aim to obtain simulation results as close as possible to the in-situ measurements data. Thus, the RS data is the input of the model, the in-situ data is the target which is the output of the model, and the model simulated results are called ANN1 and ANN2. Because there are two versions of the input RS dataset, version one (ANN1) is with parameters RS chlorophyll-a, SPM, and water temperature; and version two (ANN2) is with parameters chlorophyll-a, estimated turbidity (the turbidity calculated from RS chlorophyll-a and RS SPM), and water temperature. The input values of the two versions will be separately imported into the model with the target value (output) for

training. After the model training is completed, the simulated test data was compared with the target value to see which version of the simulated test value has better performance.

MATLAB was used as the software to build the ANN model. Firstly, the collected data after fining was imported into MATLAB, through the visualization of the plots, the relations between input-output for each parameter and the correlation between input parameters could be interpreted. The next was to normalize the feature and transform the output data. In this case, used log transformation to initial target (output data) to make the data more uniform and distributed and less centered around very low values. For input data, to remove the outliers, and divided the range of data, normalized input data between 0-1 to make sure all the inputs have the same weight, aim to accelerate the training.

3.6.2 Build and run model

After the visualization and normalization of the data, the next step was to initiate and train the ANN model. A shallow network with one hidden layer was created, the selected type of network is feedforward backpropagation. The default neuron number was 7, due to neuron number being crucial to the simulation result, it will adjust during the simulation stage. As mentioned before, the collected data were randomly split into 50% training set, 20% validation set, and 30% testing set in MATLAB. The default train function is "trianlm", the default transfer function is "logsig", and the performance function was set as MSE. Run the model after finishing all the model initiation (weight and biases), then the model performance could be seen by visualizing the regression graph of the testing and validation datasets. If the R > 0.9, it means the model most probably provides a satisfactory result.

Within the training function, "trainlm" is a network training function that updates the values of weight and bias based on Levenberg-Marquardt optimization. This algorithm is usually the fastest method for training moderate-sized feedforward neural networks, even though it normally takes more memory than other algorithms. "trainbr" is Bayesian regularization backpropagation that updates the weight and bias values according to Levenberg-Marquardt optimization. It takes longer but may be better for challenging problems. A transfer function is a method of modeling the response of a phenomenon using input and output parameters, which calculates the output of a layer based on its net input. "logsig" is the most commonly used transfer function, and the formula is shown in Equation (6)) (Dorofki et al., n.d.). "logsig" takes an input (which can have any value between positive and negative infinity) and compresses the output into a range from 0 to 1. "tansig" is a hyperbolic tangent transfer function that could run faster than other functions and have very small numerical differences. "poslin" is a positive linear transfer function, it has higher efficiency and shows better convergence performance.

$$logsig(n) = \frac{1}{1 + e^{-n}} \tag{6}$$

3.6.3 Model adjustment and visualization

This stage is to adjust the model and improve the ANN model performance, through the comparison of the RMSE result of the training and validation set to find the most desired model simulation result. The lower the RMSE, the better the fitting ability of the model. Besides, it is better to choose a model that has a smaller RMSE of the

training set than that of the validation set. To improve the model, the common approaches include (a) adjusting the number of neurons in the hidden layer (Figure 6), (b) changing the transfer function (i.e., “tansig”, “purelin”), (c) changing the algorithm (i.e., “trainim”), (d) increasing the number of hidden layers, and (e) increase the iteration number.

As introduced before, the default setting of the ANN model is one hidden layer with 7 neurons, data division for 70% training, 15% validation, and15% testing, “logsig” as the transfer function and “trianlm” as the training function. On basis of the default setting, several changes were carried out for obtaining a better-simulated result (Table 2). After visualizing the prediction from the ANN model, the model was confirmed as the one with the best simulation result (Table 3). Then, extract the simulated testing data to compare with the original target testing set to evaluate the model performance.

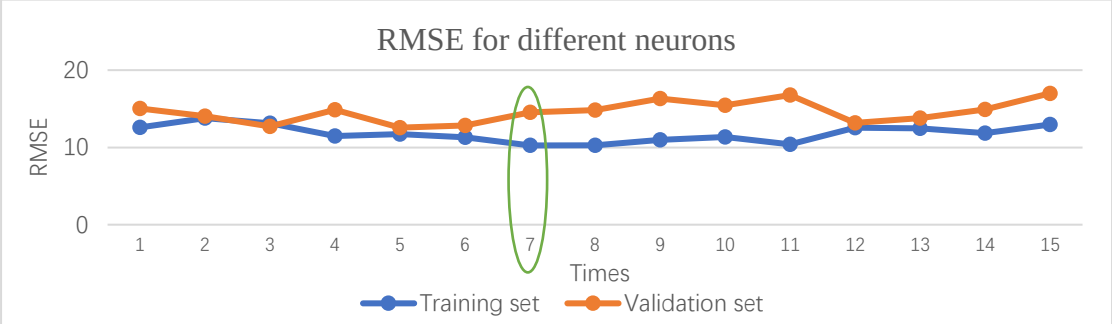

Figure 6 - Compare the RMSE of training set and validation set to find the desired neuron numbers for hidden layer

Table 2 - Changes of prediction accuracy under different scenarios of ANN model

Scenarios	***Changes to***	***Evaluation by RMSE***	
		Training set	*Validation set*
Default setting	-	**10.254**	**14.518**
Data division	70% training, 15% validation, and15% testing	16.616	14.197
Number of neurons in hidden layer	1-15 except 7	10.261	14.828
Transfer function	“poslin”, "tansig"	12.503	13.152
Train function	"trainbr"	17.888	19.372
Number of hidden layers	2-3	15.806	15.904
Iteration numbers	5000, 10000	12.900	14.947

Table 3 - The most desirable model setting after the model adjustment

Data Length	***Data divide***	***Network***	***Train function***	***Transfer function***	***Performance function***	***Hidden layer***
152	Training 50%; validation 20%, testing 30%	feedforward backprop	trianlm	logsig	MSE	1 layer, 7 neurons

4. Results

4.1 Comparison of in-situ data and RS measurement before modeling

4.1.1 The Correlation of RS and in-situ data before modeling

First, we start by looking at the consistency of in-situ data from the monitoring stations and the RS data to view their correlation and bias.

Prior to finding the correlation, these two datasets were compared by means of monthly average histograms, all histograms (Figure 7) show a seasonal distribution of each parameter. When we compare the seasonal scale, we found that the two products have a lot in common. For example, for all the three parameters, the values of these two datasets are similar on the time scale and the inter-seasonal fluctuations fit well. Especially for the water temperature parameter, the monthly average data are very similar. This is followed by chlorophyll-a and turbidity, which have some differences in values, but the seasonal fluctuations are still very consistent. In addition, the RS data fluctuated less in seasonal differences and the overall RS data are slightly lower than the in-situ data. It is reasonable because in-situ measurements are made directly in the river while RS data were located slightly off the measurement point. Especially for the parameters chlorophyll-a and turbidity, which rely on optical observations, so changes in the light, atmosphere, or the weather have a significant impact on the stability of remote sensing.

It is also worth mentioning that, from the characteristics of the parameters, the values of chlorophyll-a are higher in summer than in other seasons, the difference between the two data is also larger in summer, which may also be an effect of the variable weather in summer on RS observations. The same story occurs for turbidity, where RS measurements show the largest differences relative to in-situ measurements in both summer when the in-situ measurements have the lowest values, and in winter, when they are the highest.

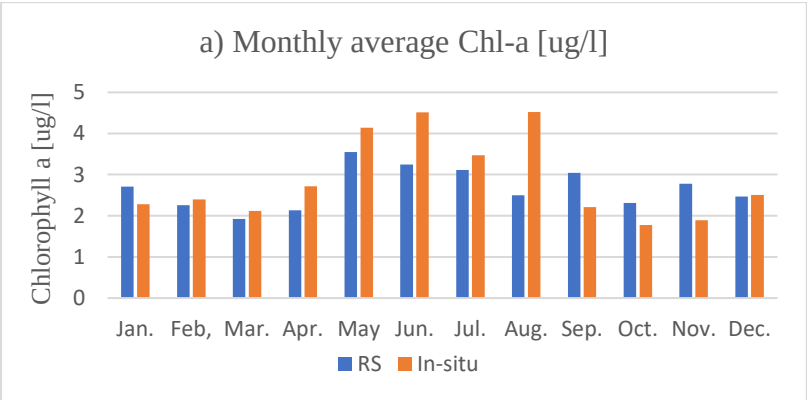

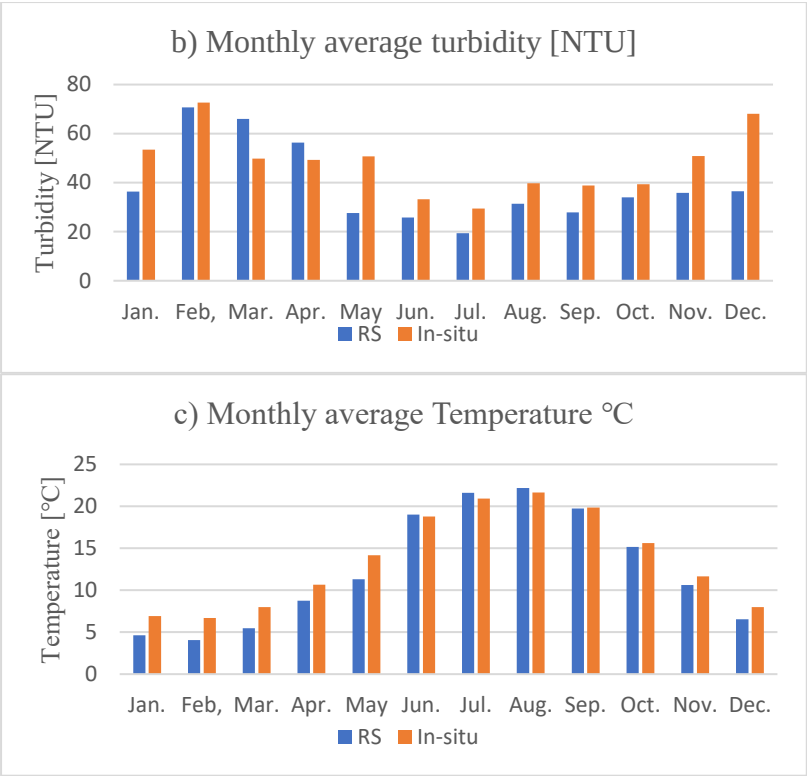

Figure 7 - Monthly average histogram for parameter a) Chl-a, b) Turbidity and c) Water Temperature

A scatter plot is a good way to quickly check correlations between consecutive data pairs. The scatter plots below show the original RS and in-situ data sets before the simulation (Figure 8). Each point on the plot represents the water quality at a given time, showing the combination of RS measurements and in-situ measurements at that time.

It can be seen the data show an uphill pattern from left to right along the x-axis, this indicates a positive relationship between the raw RS and in-situ data. Even though this relationship is not obvious, especially in the second half of the data, the points fall into a certain degree of disorder, but the overall trend is still consistent. The distribution of this scatter plot reveals the correlation between the two data sets before the simulation. Where the fit is better means the data are very concentrated, and the random occurrence of extreme data makes the two data sets much less correlated. R as the correlation coefficient is the quantitative assessment that measures both the direction and the strength of the tendency, as agree the R must > 0.9 to reach the satisfactory result, R equals 0.457 from Figure 8 confirms the poor correlation between these two original datasets.

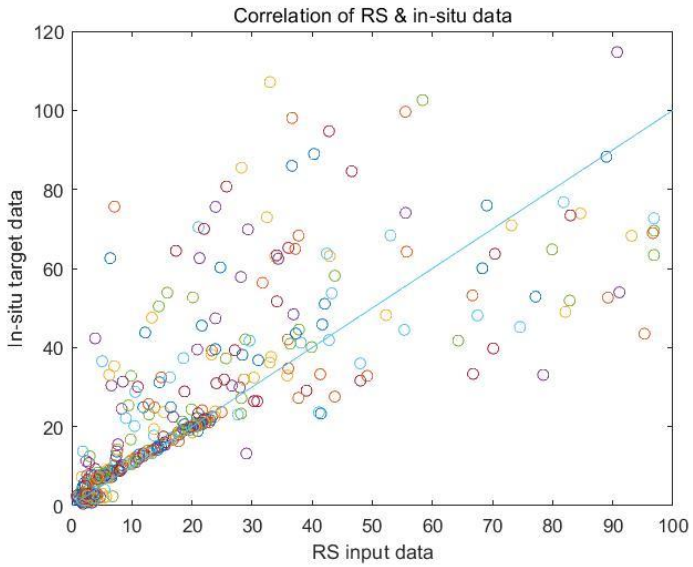

Figure 8 - The correlation plot of RS & In-situ data before modeling

In addition to observing the correlation between RS and in-situ data sets in general, it is also interesting to view the correlation between RS and in-situ data for each parameter, which can reveal the ratio of the contribution of different parameters to the overall correlation. The three correlation charts visualize the correlation between RS and in-situ data for the three parameters (Figure 9). Each point in the scatter plot represents a combination of RS measurements and in-situ measurements of a parameter at a given time. Visually, temperature has a very strong positive correlation, as the RS temperature [°C] increases, the in-situ temperature [°C] increases accordingly. While chlorophyll-a and SPM (turbidity) have very weak correlations and the data are very scattered, with only a vague trend of positive correlation. The values of their correlation coefficients R were 0.1847 for chlorophyll-a, 0.4579 for SPM, and 0.9792 for water temperature. based on the concept of Pearson's correlation coefficient, the significant high R represents the RS and in-situ water temperature has a very high correlation. Instead, even R for SPM (turbidity) indicates a positive correlation between the two variables, but the correlation was weak and possibly insignificant. While the R for chlorophyll-a is evidence that the two variables are infinitely close to no correlation.

This study also attempted to observe the correlation between each of the three parameters in the original RS datasets. To see if there was a significant linear relationship and a high correlation between the different water quality parameter pairs, there are three correlation plots to present the correlation of each parameter pair (Figure 10). The point in the scatter plot represents a combination of any two parameters from the original RS data at a given time, the correlation between any two parameters is difficult to identify. And the distribution of data points in all three scatter plots is very dispersed, with no obvious trend of increasing or decreasing one parameter with the other. In addition, when analyzing the calculated correlation coefficient values, the R between chlorophyll and SPM was 0.2311, between chlorophyll-a and the water temperature was 0.2156, and between SPM and water temperature was 0.453. A value of 0.5 indicates a weak and possibly insignificant correlation between the two variables, thus concluded that any two original RS parameters show a very weak correlation.

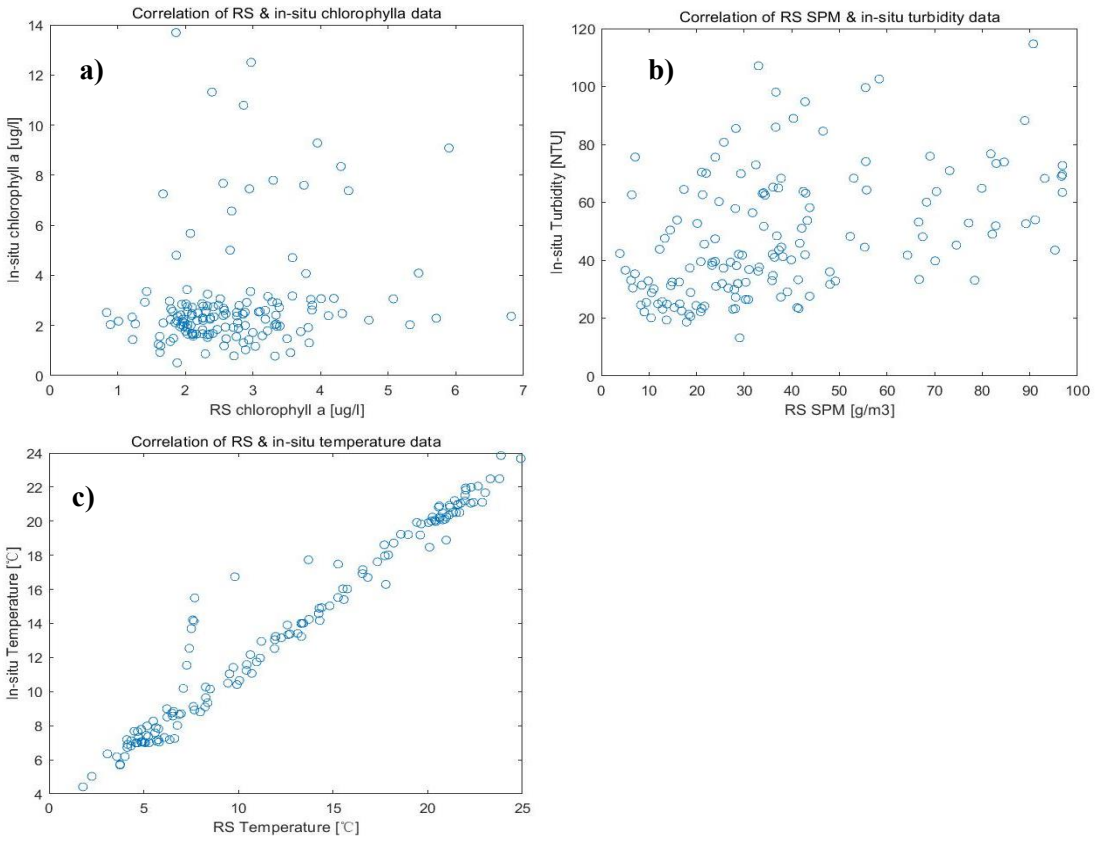

Figure 9 - Correlation plot of RS & in-situ measurements of a) Chl-a, b) SPM & turbidity and c) water temperature before modeling

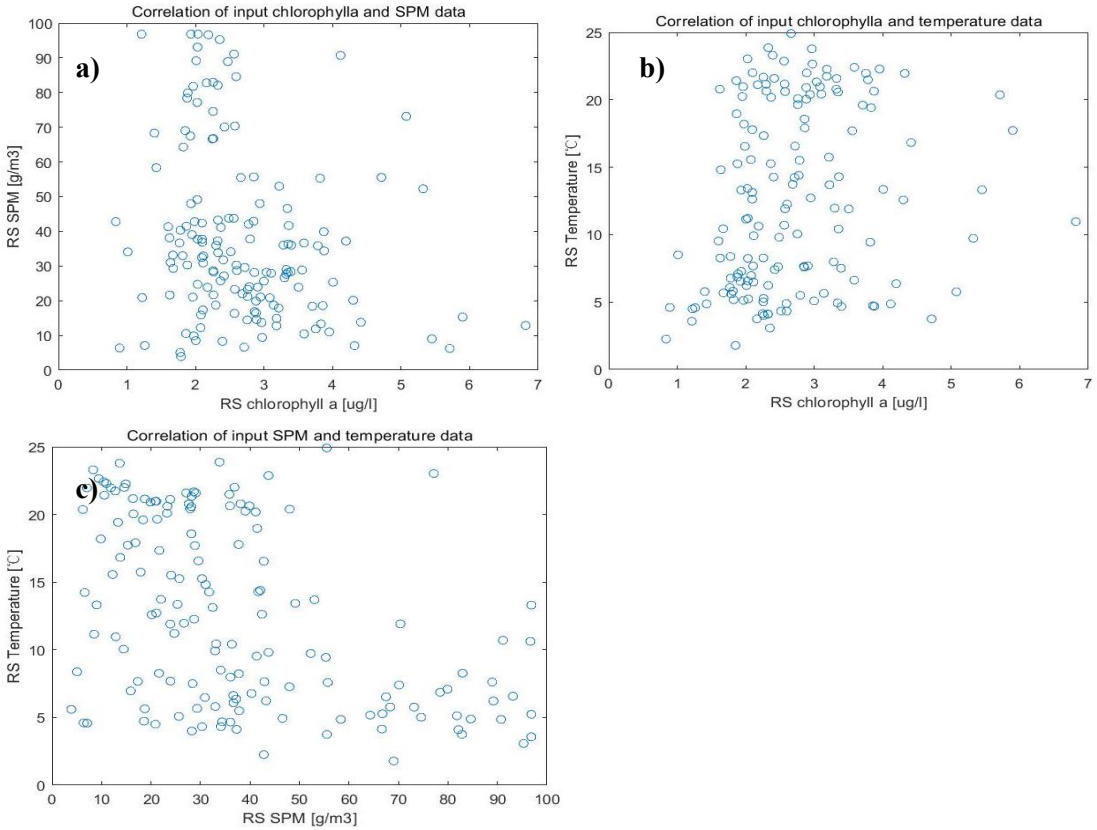

Figure 10 - Correlation plot of two RS parameters a) Chl-a & SPM, b) Chl-a & water temperature and c) SPM & water temperature before modeling

4.2 The ANN model performance visualization

In this stage, the model performance was interpreted by observing the correlation between target data (in-situ) and the simulated data. From the overall view, comparing the R for each stage of the two models (Table 4), the R of both ANN models are very high in the training, simulation, and testing sets. This means that they all exceed the criterion of R=0.95 which represents the most satisfactory simulation results. From another perspective, as the fitted line equation is given in the regression plot, (assuming the equation y = ax + b), the a and b coefficients are closer to 1, and 0 have higher R values (Kisi, 2013).

When looking at the regression plots (Figure 10, Figure 11), the colored line in each graph shows the ideal output. These points tell how well the model is generalizing, the more the points lie on the line, the better the regression result is. Compared to the two models, it was found that the simulation result of ANN2 is better because it has a slightly higher R in the test set and the full dataset than ANN1. The reason might be that the estimated turbidity as an input value is more correlated with the target value of the model (in-situ data) than SPM as an input value, due to it is a combination of chlorophyll-a and SPM.

Table 4 - Training, validation, and testing regression results of the ANN models with different input combination

	R	
	ANN1*(with input SPM)*	***ANN2*** *(with estimated turbidity)*
Training	0.978	0.972
Validation	0.963	0.959
Testing	0.932	0.963
All	0.961	0.966

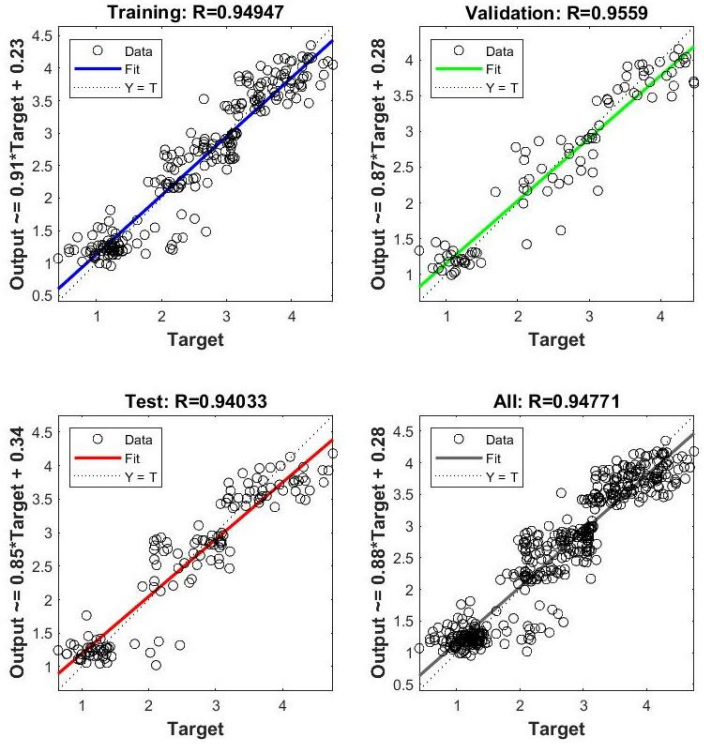

Figure 10 - The regression plot of simulated RS data (ANN1 - with SPM, Chl-a and water temperature as original input data) vs. the in-situ observation (target)

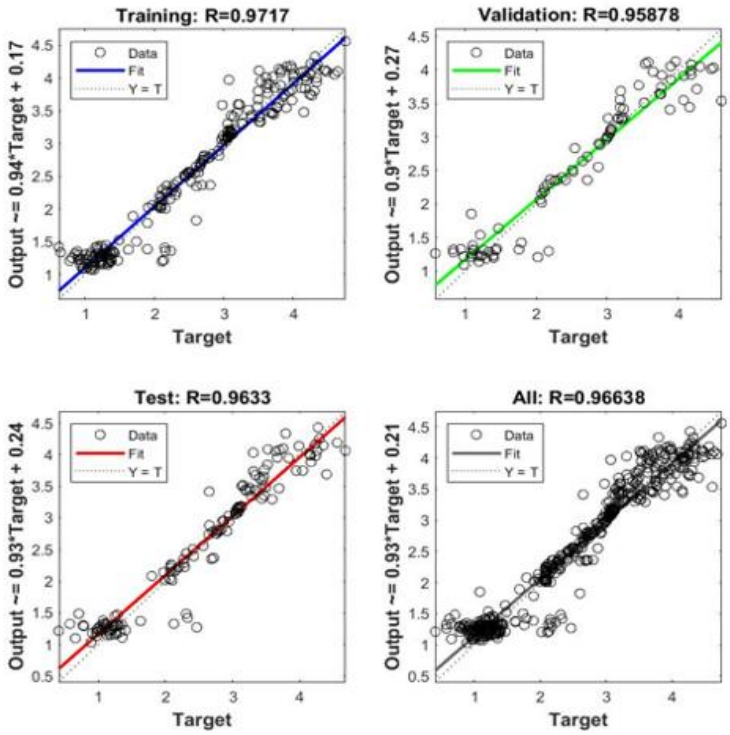

Figure 11 - The regression plot of simulated RS data (ANN1 - with estimated turbidity, Chl-a and water temperature as original input data) vs. the in-situ observation (target)

The next point worth emphasizing is the analysis of the ANN model simulation capability. While interpreting the following correlation map (Figure 12, Figure 13), the x-axis is the predicted chance of the three water quality parameters, the y-axis is the original in-situ measurements of the three water quality parameters. The marker "x" represents the training set, "o" represents the validation set, and "▽" is the marker of the testing set. Besides, the training and validation sets are in black, and the testing set is in red. These points tell how well the model is generalizing, the far the point to the dialogue line, the less good model is. The results show the correlation between the simulated RS data and the target in-situ data is much better than before the simulated in the model. One of the phenomena is that the points of the larger data are not as scattered as before the simulation, and the data distribution has become more concentrated. This is mainly due to the better simulation result of SPM (turbidity), as its value is relatively bigger than other parameters.

When comparing the simulation capabilities of the two models, ANN2 is clearly better for the simulated result higher than 25, as the data are more concentrated and evenly distributed over the fitted line. For values above 25, the difference is not particularly pronounced, however, it can be observed that the model ANN2 has fewer extreme values, and the data points are slightly less spread than ANN1. Therefore, the overall performance of the ANN2 model is better than that of ANN1.

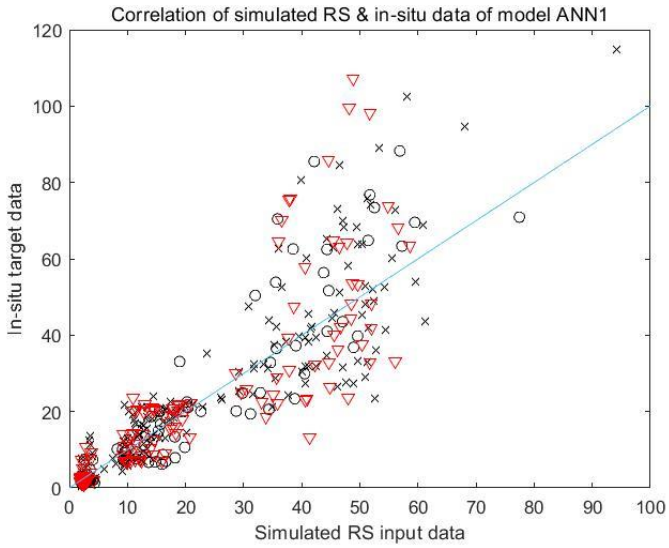

Figure 12 - Visualize the prediction of the ANN model (ANN1 - with SPM as original RS data)

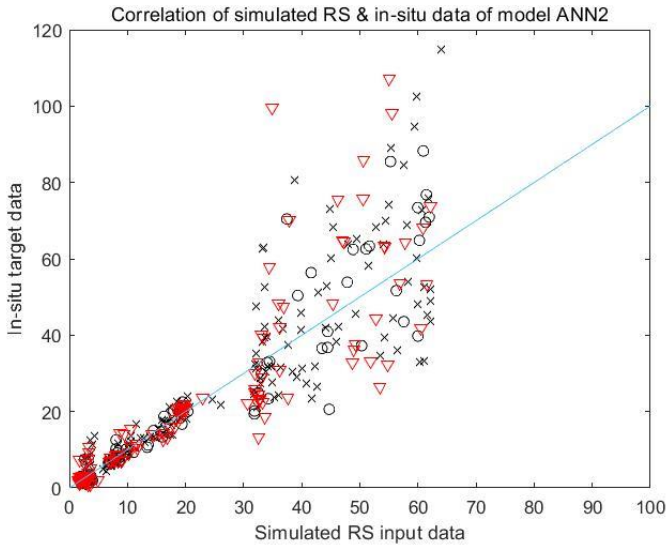

Figure 13 - Visualize the prediction of the ANN model (ANN2 - with estimated turbidity as original RS data)

4.3 The ANN model evaluation

After repeated training to successfully constructed the two ANN models, four quantitative statistics were introduced as model evaluation parameters (R^2, RMSE, MAE, PBAIS). The aim is to determine the goodness of fit and evaluate the ANN models from the perspectives of covariance, normalization, and error (D. N. Moriasi et al., 2007). Changes in the input parameters of the ANN can lead to differences in the simulation results, and the performance of the model is compared by the differences in the model estimation parameters (Figure 14).

Visually, ANN2 has a higher R^2 and relatively lower values in the error indices (MAE, RMSE and PBAIS), which indicates that the ANN2 model simulates the data better and performs better. From the R^2 point of view, both models have satisfactory results in the simulation of water temperature ($R^2 > 0.8$). However, they do not achieve acceptable results in the simulation of chlorophyll-a and turbidity, and it is difficult to distinguish the expressiveness of the two.

To explain the error metrics RMSE and MAE, a perfect match is indicated when the value of RMSE is 0, and the correlation can be considered low if an RMSE value less than half of the standard deviation. Unfortunately, the RMSE of both models for chlorophyll-a and turbidity slightly exceeded this criterion, and only the RMSE of water temperature gave acceptable results, but the relative ANN1 overall RMSE performed slightly better than ANN1. Second, the NSE ranges between ∞ and 1.0, with NSE =1 being the optimal value, so there is no doubt that the ANN2 model with NSE closer to 1 for all three parameters performs better. For PBAIS, if it is below 25% in the model for flow, the model simulation is judged as satisfactory, so both models are satisfactory. Especially for chlorophyll-a and turbidity where a significant reduction in PBAIS of ANN2 can be seen, it indicates the superiority of the ANN2 model. It also can be seen the PBAIS has a slight increase in water temperature, this is probably due to the compromise made in the simulation to optimize weights and errors.

The results show that the model performance varies for scenarios with different input parameters. if we rated the model performance by 4 criteria from high to low "Excellent", "Satisfied", "Good" and "Unsatisfied", the data and ratings of models can be seen in the following table (Table 5).

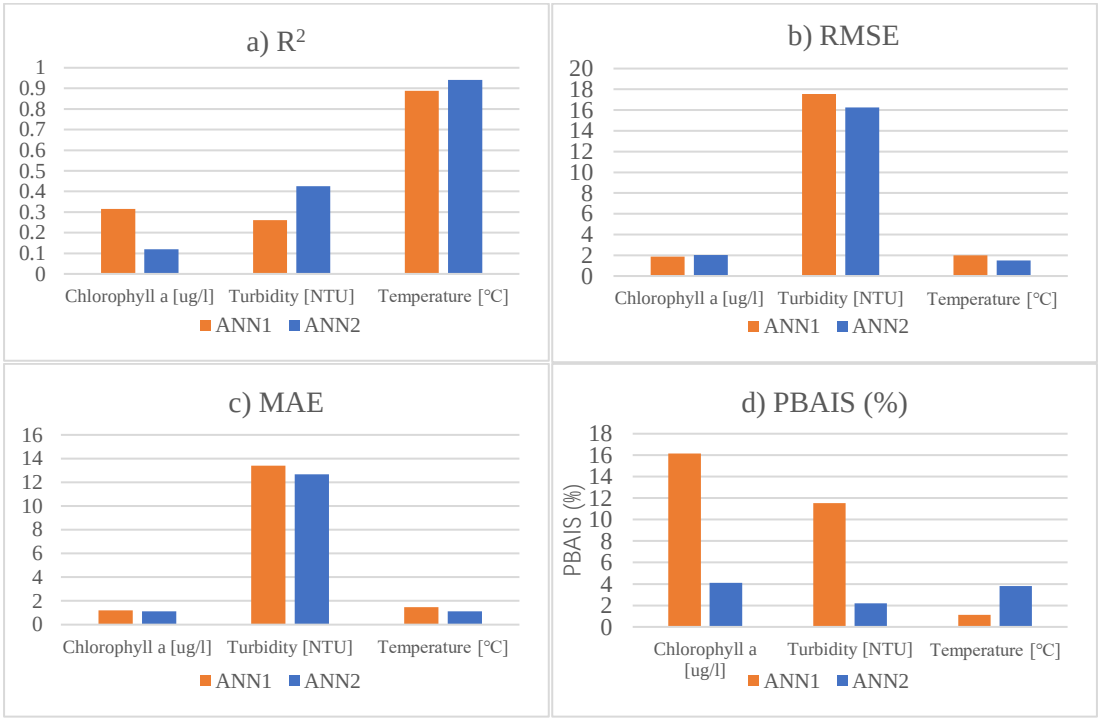

Figure 14 - Histograms comparing ANN model performance by model evaluation parameters a) R^2, b) RMSE [ug/l] or [NTU] or [℃], c) MAE [ug/l] or [NTU] or [℃], and d) PBAIS (%)

Table 5 - Comparison of the ANN model performance of the water quality parameters

Model	***Parameters***	***Model performance***				***Performance rating***
		R^2	*RMSE*	*MAE*	*PBAIS (%)*	
ANN1	Chl-a [ug/l]	0.314	1.865 [ug/l]	1.214[ug/l]	16.159	Good
	Turbidity [NTU]	0.261	17.552 [NTU]	13.412[NTU]	11.536	Good
	Temperature [℃]	0.889	1.983 [℃]	1.474 [℃]	1.115	Excellent
ANN2	Chl-a [ug/l]	0.119	2.030 [ug/l]	1.135 [ug/l]	4.116	Good
	Turbidity [NTU]	0.425	16.237 [NTU]	12.682 [NTU]	2.202	Satisfied
	Temperature [℃]	0.941	1.507 [℃]	1.112 [℃]	3.816	Excellent

5. Discussion

This study is a practical solution for estimating water quality in the Schelde estuary by ANN using remote sensing images and in-situ measurements. The combination of temporal and spatial flexibility of the RS images, and the nonlinear estimation capability of the ANN, allow the obtained results to give more accurate estimates than classical regression methods (Damme et al., 2005). Confirming the superior ability of the nonlinear model structure of neural networks for water management.

In general, phytoplankton suspended particles and dissolved organic matter in coastal and inland waters contribute significantly to the optical properties (Salman et al.,2013), which makes RS observations with optical lenses difficult. The results of this study also showed significant differences between in situ and RS monitoring and a low correlation between the data (R = 0.457). Therefore, it is highly expected the ANN model can reduce the bias in the previous results. Compared to the results in Table 6, it can be found that the use of the neuron network model can predict the water quality data provided by in-situ measurements from MODIS images very well. Changing the input environmental variables can also improve the predictive power of the model on the original basis.

Table 6 - Pearson's correlation coefficient (R) between in-situ data and RS data and ANN prediction RS data

	Inputs RS parameters	***Correlation coefficient***	***Overall correlation coefficient***
In-situ VS. RS data	Chlorophyll-a	0.185	0.457
	Estimated turbidity	0.458	
	Water temperature	0.979	
ANN1	Chlorophyll-a	0.334	0.961
	SPM	0.558	
	Water temperature	0.706	
ANN2	Chlorophyll-a	0.356	0.966
	Estimated turbidity	0.592	
	Water temperature	0.946	

5.1 Station-wise accuracy of RS measurement

The RS measurement and in-situ measurement in the monitoring station datasets matched very well in describing water temperature, and the trends in describing chlorophyll-a concentrations and turbidity statistics were generally consistent. However, the data did not match well. When the bias is analyzed in terms of station matching and specific environmental factors, the greatest under- and overestimation of the RS data can be seen during spring and midsummer bloom (Apr. to Aug.) (Figure 7). Especially for chl-a, when rapid changes in its concentration are typical, which can also affect turbidity estimates. Part of the underestimation for chl-a and turbidity can be explained by the apparent difference in the specific absorption spectra of phytoplankton measured in spring and summer, which may be related to the spring flowering period when chl-a concentrations are higher. Besides, many of the visible differences between RS chl-a and turbidity with their in-situ measurements can be explained by the large differences

in sampling volume. Due to the monitoring volume and detection range of RS are larger than those of the site measurements (Attila et al., 2018), RS measurement is 5min data instead of weekly data as in-situ measurement. In addition, the influence of weather factors such as cloud cover and rain on the stability of RS monitoring is not negligible.

Several authors have used satellite image data to observe numerical coefficients such as chlorophyll-a in water quality mapping. Salman et al. (2013) have demonstrated moderate agreement between MODIS and in-situ chlorophyll data. When comparing in-situ measurements of water quality parameters with RS, the optimal regression model of Gohin (2011) produced an R^2 of 0.92 for chl-a, and the best model yielded regression coefficients is 0.94 and 0.97 for turbidity and SPM, respectively. Chuanmin Hu et al. (2004) also attempted to use MODIS satellite data to estimate chl-a concentrations in Tampa Bay, the agreement between the RS data and the in-situ measurements was called strong ($R^2 = 0.72$). However, in this study, R^2 was only 0.0341 for chlorophyll-a, and 0.2097 for SPM (Figure 9), values of R^2 which were much lower than expected. In addition to the reasons mentioned above regarding phytoplankton, greater monitoring volume, and the influence of weather, a greater influence is the location of the monitoring sites. Due to the limited resolution of the RS product (1km X 1km), the coordinates are not exactly the same when locating the in-situ monitoring sites on the RS images. The location was more westward and biased towards the estuary, so it is speculated that the offset of the coordinates is one of the most important factors for the very low fit of the RS and in-situ data. In addition, it does not have much effect on the fit of water temperature, because the water temperature does not change significantly for the river spatially (Chebud et al., 2012).

Furthermore, to obtain higher quality RS data in complex estuaries, it is suggested to (1) a sufficient number of in-situ measurements for the selected water quality, as well as a longer time span, (2)improve the accuracy of the positioning of the monitoring points and try to select highly resolved RS products, (3) have knowledge of each selected pixel point on the RS image, such as information on phytoplankton types within the water body, and (4) for estuaries, improve the accuracy of RS algorithms targeting chl-a or turbidity concentrations (Attila et al., 2018).

5.2 The performance of the ANN model

Nonlinear neural network models can produce more accurate estimates than traditional methods, especially when the model is trained without dense data available. The ANN model does not need to know the parameter relationship in advance, and it has the ability to consider the nonlinear multi-parameter relationship between the reflectivity and water quality parameters (Ceyhun & Yalçın, 2010).

When processing the data input to the model, the RS data was collected from The Copernicus Marine Service (CMEMS) satellite imagery, which had been preprocessed for geometric correction. However, it only provides SPM products instead of turbidity. In order to ensure consistency among all variables, this study decided to obtain estimated turbidity from known chlorophyll-a and SPM in CMEMS (Gohin, 2011). Derivatives of this type of satellite data are imperfect but can be locally assessed by comparison with in-situ observations, even if the satellite data input to the model differs significantly from in situ observations.

The two ANN models constructed in this study have different input parameters, ANN1 is the same as the original SPM data, and ANN2 replaces the original SPM data with estimated turbidity data. After the successful construction of the model, the coefficient of determination R^2 obtained by the graph fitting of the observed and

simulated results are all above 0.95. Figure 12 presents the fitting results of the two models respectively, showing good agreement between the monitored and simulated values. The result reveals this method can be used as a suitable technique to predict the water quality data of the Schelde estuary. And the results also confirmed the speculation that the simulation results would be different when the parameters of the ANN were changed. The results show that under different parameter scenarios, the R^2 is different between the measured and simulated water quality parameters, and the ANN2 model has higher performance.

This is because the simulation results of water turbidity prediction are more sensitive to the transfer function of the hidden layer and the transfer function of the output layer than other parameters (Chang & Liao, 2012). When adjusting the model settings, we tested the three transfer functions of "logsig", "poslin" and "tansig" respectively. The simulation results verified the theory proposed by Chang et al. (2012) that an incorrect transfer function would increase the simulation error. Finally, the "logsig" with the smallest RMSE was selected as the transfer function of the model in this study. In addition, this study also found that the simulation results of the two ANN models are more sensitive to the parameter "number of hidden layers" than the "Number of hidden layers" and "iteration number" parameters. When training the model, it is found that the simulation results vary a little in each calculation process, but the variation is within an acceptable range (Salman et al.,2013). ANN models have the advantage of having multiple tunable parameters and configurations, understanding the functions and differences of the various settings of the ANN model can help avoid unnecessary parameter training processes and obtain a better-fit observation.

ANN models are sensitive to different input variables (Wang et al., 2013), thus it is interesting to compare the ANN models performance for each water quality parameter (Table 5). The modeling results show that the R for chl-a and turbidity are relatively low, all of them are below R = 0.5, so it is difficult to be considered as a valid fit. But the results are still better than the RS data for chl-a and turbidity before modeling, which is a significant improvement over the simulated results. And the water temperature plays as stable as ever on R, which is very high (R<0.8) as well as the RS data before the simulation. In addition to this, as mentioned earlier, RMSE values less than half the standard deviation of the measured data can be considered as low. While the RMSE of chlorophyll-a and turbidity of both models slightly exceeded this criterion, only the RMSE of water temperature gave acceptable results. Although the RMSE of ANN2 for each water quality parameter performed slightly better than ANN1, indicating that the ANN2 model gave fewer differences between predicted and observed data.

ANN model can achieve high R^2 values, especially for total cyanobacterial populations, however unfortunately they do not provide an explicit description of the underlying processes (Recknagel et al., 1997) (Chebud et al., 2012). The regression coefficient R^2 for Chl-a of the constructed ANN model is just above 0.95, and the R^2 of the Chl-a simulation with ANN model in the lake Baiyangdian is 0.72 (Wang et al., 2013). Through the sensitivity analysis of ANN model by (Chang & Liao, 2012), the R^2 of measured and estimated water turbidity are 0.88 for the training set and 0.64 for the validation set. Although R and R^2 have been widely used for ANN model evaluation, it still has limitations. Especially since their data are too sensitive to high extremes, and insensitive to additive scale differences between model predictions and measured data (Salman et al., 2013). Moreover, it has been pointed out by scientists that data preprocessing is crucial for the success of ANN training (Wilson & Recknagel, 2001) (Wang et al., 2013). This idea was also validated in the model training session of this study. Where the RS input data were processed to normalize them and the target data

were transformed to ensure that all inputs had the same weights, which indeed accelerated the training time and improved the accuracy of the fit.

In conclusion, ANN as a data-driving model requires less prior knowledge in the development process, which is its advantage. However, this also leads to a strong reliance on the availability and quality of data for this model, and data that are not appropriate to the model's simulation goals or are not properly preprocessed can lead to severe limitations in model performance (Rousso et al., 2020b).

6. Conclusion & Recommendations

6.1 Conclusion

In the past 20 years, ANN has been applied in many water resources and engineering research, and the nonlinear, model-free structure of ANNs can produce more accurate estimates than classical regression methods. This study discusses the simulation of RS data in the modeling phase and some optimization issues involved. Remote sensing (RS) was used to monitor the water quality parameters of the Scheldt Estuary, an artificial neural network (ANN) method was introduced, and it was applied to the RS data. Then the simulation results were compared with the field measurements to check the model performance. The purpose is to rely on the training and optimization of the artificial neural network model, so that the input remote sensing (RS) data can obtain simulation results as close as possible to the in-situ measurement data. A brief comparison of the results approved that the ANN model can well predict the chlorophyll-a concentration, turbidity, and water temperature in the estuary from satellite data, showing its potential in water quality modeling. In addition, due to the different versions of the input dataset (RS products), we found that as input, the numerically calculated turbidity data can improve the performance of the simulated ANN model compared to the SPM data.

Based on the process and results of this study, several key steps are summarized to obtain better simulation data, i.e., data with a better fit to the target data. The first is the selection of water quality parameters, which determines the overall predictive ability of the model on the water quality of the study site. For example, this study uses three parameters for the characteristics of estuarine water quality: chl-a, turbidity, and water temperature, not the more parameters the better the simulation effect, but to choose the appropriate parameters according to the actual local geomorphology and conditions. And, to consider the availability of RS products, there are many papers to support the water quality parameters are the most guaranteed.

Second, it is the collection and pre-processing of data. Especially since ANN is a data-driven model, the quality of the data input to the model directly determines the upper limit of the model's performance. It is recommended to choose the longest possible time span and representative data. For RS data, we should try to choose RS products with high resolution and improve the accuracy of positioning for in situ monitoring points. The accuracy of the algorithm of RS products for different parameters plays a decisive role, sufficiently sensitive spatial sensors and more accurate atmospheric correction schemes are also very helpful to improve the performance of the model.

The third point is the selection of model input parameters, which in this study represent the chl-a, estimated turbidity (or SPM), and water temperature as the original input values of the ANN model. The ANN model is very sensitive to different input variables, careful selection of input parameters and preprocessing of parameters can help improve the performance of the model. In addition, selecting parameters with more obvious correlations can also make the results fit better. In this study replacing the original SPM of the input data bin of the model with the turbidity estimated according to chl-a and SPM significantly improves the performance of the model.

Last but not the least, the construction and training of ANN models. The ANN behaves like a human neuronal system, and the simulation results are variated in each attempt within an acceptable range. It is known that ANN models have the advantage of multiple adjustable parameters and configurations, so adjusting the configuration of

the model can obtain better fitting results. Such as the number of neurons in the hidden layer, the transformation equation, etc.

The temporal and spatial flexibility of remote sensing images and the nonlinear estimation capability of artificial neural networks are the main advantages. This study demonstrates the feasibility of marine observation remote sensing products for routine monitoring of narrow waterways, and the usefulness of ANN models in simulating water quality, especially for practical applications in scenarios such as estuaries.

6.2 The future expectations

Due to time constraints, this study does not show a comprehensive modeling water quality analysis case. There is still much room for improvement and exploration in some fields, such as data adoption, selection of water quality parameters, satellite sensor type, and suitable optical algorithm selection, etc.

In terms of data adoption, this study only analyzed three years of weekly water quality data, because of the limitation of the sample size and time length of the available in situ data. Besides, a longer period should be studied to better determine the trend of water quality in the water body with the seasons and the treatment of water quality in recent years. In addition, multiple monitoring stations (pixels in satellite images) should be introduced, instead of just one station (one study point). Because more data can improve the accuracy of the model and can also help analyze the spatial variation of water quality. Furthermore, try to look at the monthly average simulation data from the ANN model on a time scale, this could help to see if there is a difference in the accuracy of the model simulation results over the seasons.

In terms of water quality parameters, to study local water quality changes, a 3-year study period is quite limited, and we need longer-term continuous monitoring data. Besides, more samples of water quality parameters can be collected to analyze the impact of other water quality parameters on water quality. This helps to observe the relationship between different parameters to see if the correlation between the parameters will affect the fitting ability of the model. In addition, the nutrient limitation is not common in most of the Shelter estuary, and light is the main limiting factor for phytoplankton growth (Damme et al., 2005). Phytoplankton in the estuary is an important link in the food web, playing a critical role in elemental cycling, water quality, and food supply. Thus, it is important to understand how it is transferred to higher trophic levels (Damme et al., 2005). Although the study period is relatively short, it can still help to manage water quality in estuaries more efficiently if multiple mechanisms of variability can be sorted out and anthropogenic influences can be separated from natural variability.

The dilemma encountered in the selection of remote sensing products is that monitoring of estuarine and coastal water quality parameters requires repeated and frequent synoptic-scale observations. However, most satellite sensors lack sufficient spatial resolution, proper sensitivity, and calibration (Morel & Prieur, 1977). In addition, there is no reliable algorithm for relevant water quality parameters, and complex data processing is an obstacle to the observation of estuarine water quality by marine satellite products (Hu et al., 2004). Since current instruments with a high spatial resolution such as The Operational Land Imager (OLI) and Multi-Spectral Instrument (MSI), they are mainly designed for ground-based observations. It is recommended to apply sensors with a higher spatial resolution for sub-mesoscale processes in coastal areas (Werdell et al., 2018). The MODIS data used in the study provided sufficient resolution (1 km) and sensitivity to observe medium-sized estuaries, and Ocean Colour products provided

appropriate bio-optical algorithms, making it possible to obtain reliable water quality parameters. However, the fitting of chlorophyll-a and turbidity to the in-situ measurements obtained in this study is not very good, so further research is needed to evaluate the method. Perhaps using images from other available satellite sensors to Achieve better estimates and looking forward to more appropriate bio-optical algorithms and calibration strategies.

In the end, the effectiveness of neural networks as a predictive tool has not yet been fully resolved. For example, some studies have used many environmental parameters as input variables without considering the best choice among them (Chau & Cheng, 2002), therefore, this technology deserves more work in water resources monitoring.

7. References

A logical calculus of the ideas immanent in nervous activity | SpringerLink. (n.d.). Retrieved June 7, 2022, from https://link.springer.com/article/10.1007/BF02478259

A Water Quality Index for River Management—HOUSE - 1989—Water and Environment Journal—Wiley Online Library. (n.d.). Retrieved June 7, 2022, from https://onlinelibrary-wiley-com.kuleuven.e-bronnen.be/doi/abs/10.1111/j.1747-6593.1989.tb01538.x

AL-Fahdawi, A. A. H., Rabee, A. M., & Al-Hirmizy, S. M. (2015). Water quality monitoring of Al-Habbaniyah Lake using remote sensing and in situ measurements. *Environmental Monitoring and Assessment*, *187*(6), 367. https://doi.org/10.1007/s10661-015-4607-2

Altunkaynak, A. (2007). Forecasting Surface Water Level Fluctuations of Lake Van by Artificial Neural Networks. *Water Resources Management*, *21*(2), 399–408. https://doi.org/10.1007/s11269-006-9022-6

Attila, J., Kauppila, P., Kallio, K. Y., Alasalmi, H., Keto, V., Bruun, E., & Koponen, S. (2018). Applicability of Earth Observation chlorophyll-a data in assessment of water status via MERIS — With implications for the use of OLCI sensors. *Remote Sensing of Environment*, *212*, 273–287. https://doi.org/10.1016/j.rse.2018.02.043

Baeyens, W., van Eck, B., Lambert, C., Wollast, R., & Goeyens, L. (1998). General description of the Scheldt estuary. In W. F. J. Baeyens (Ed.), *Trace Metals in the Westerschelde Estuary: A Case-Study of a Polluted, Partially Anoxic Estuary* (pp. 1–14). Springer Netherlands. https://doi.org/10.1007/978-94-017-3573-5_1

Billen, G., Garnier, J., & Rousseau, V. (2005). Nutrient fluxes and water quality in the drainage network of the Scheldt basin over the last 50 years. *Hydrobiologia*, *540*(1–3), 47–67. https://doi.org/10.1007/s10750-004-7103-1

Ceyhun, Ö., & Yalçın, A. (2010). Remote sensing of water depths in shallow waters via artificial neural networks. *Estuarine, Coastal and Shelf Science*, *89*(1), 89–96. https://doi.org/10.1016/j.ecss.2010.05.015

Chang, C.-L., & Liao, C.-S. (2012). *Parameter Sensitivity Analysis of Artificial Neural Network for Predicting Water Turbidity*. *6*(10), 4.

Chau, K. W., & Cheng, C. T. (2002). Real-Time Prediction of Water Stage with Artificial Neural Network

Approach. In B. McKay & J. Slaney (Eds.), *AI 2002: Advances in Artificial Intelligence* (pp. 715–715). Springer. https://doi.org/10.1007/3-540-36187-1_64

Chebud, Y., Naja, G. M., Rivero, R. G., & Melesse, A. M. (2012). Water Quality Monitoring Using Remote Sensing and an Artificial Neural Network. *Water, Air, & Soil Pollution*, *223*(8), 4875–4887. https://doi.org/10.1007/s11270-012-1243-0

D. N. Moriasi, J. G. Arnold, M. W. Van Liew, R. L. Bingner, R. D. Harmel, & T. L. Veith. (2007). Model Evaluation Guidelines for Systematic Quantification of Accuracy in Watershed Simulations. *Transactions of the ASABE*, *50*(3), 885–900. https://doi.org/10.13031/2013.23153

Damme, S. V., Struyf, E., Maris, T., Ysebaert, T., Dehairs, F., Tackx, M., Heip, C., & Meire, P. (2005). Spatial and temporal patterns of water quality along the estuarine salinity gradient of the Scheldt estuary (Belgium and The Netherlands): Results of an integrated monitoring approach. *Hydrobiologia*, *540*(1–3), 29–45. https://doi.org/10.1007/s10750-004-7102-2

Directive 2008/56/EC of the European Parliament and of the Council of 17 June 2008 establishing a framework for community action in the field of marine environmental policy (Marine Strategy Framework Directive) (Text with EEA relevance), EP, CONSIL, 164 OJ L (2008). http://data.europa.eu/eli/dir/2008/56/oj/eng

Dorofki, M., Elshafie, A. H., Jaafar, O., & Karim, O. A. (n.d.). *Comparison of Artificial Neural Network Transfer Functions Abilities to Simulate Extreme Runoff Data*. 6.

Gholizadeh, M., Melesse, A., & Reddi, L. (2016). A Comprehensive Review on Water Quality Parameters Estimation Using Remote Sensing Techniques. *Sensors*, *16*(8), 1298. https://doi.org/10.3390/s16081298

GlobColour—Home. (n.d.). Retrieved June 1, 2022, from https://hermes.acri.fr/

Gohin, F. (2011). Annual cycles of chlorophyll-<i>a</i>, non-algal suspended particulate matter, and turbidity observed from space and in-situ in coastal waters. *Ocean Science*, *7*(5), 705–732. https://doi.org/10.5194/os-7-705-2011

Govindaraju, R. S. (2000). Artificial neural networks in hydrology. II: hydrologic applications. *Journal of Hydrologic Engineering*, *5*(2), 124–137.

Gupta, H. V., Sorooshian, S., & Yapo, P. O. (1999). Status of Automatic Calibration for Hydrologic Models: Comparison with Multilevel Expert Calibration. *Journal of Hydrologic Engineering*, *4*(2), 135–143. https://doi.org/10.1061/(ASCE)1084-0699(1999)4:2(135)

Hameed, M., Sharqi, S. S., Yaseen, Z. M., Afan, H. A., Hussain, A., & Elshafie, A. (2017a). Application of artificial intelligence (AI) techniques in water quality index prediction: A case study in tropical region, Malaysia. *Neural Computing and Applications*, *28*(S1), 893–905. https://doi.org/10.1007/s00521-016-2404-7

Hameed, M., Sharqi, S. S., Yaseen, Z. M., Afan, H. A., Hussain, A., & Elshafie, A. (2017b). Application of artificial intelligence (AI) techniques in water quality index prediction: A case study in tropical region, Malaysia. *Neural Computing and Applications*, *28*(S1), 893–905. https://doi.org/10.1007/s00521-016-2404-7

Hu, C., Chen, Z., Clayton, T. D., Swarzenski, P., Brock, J. C., & Muller–Karger, F. E. (2004). Assessment of estuarine water-quality indicators using MODIS medium-resolution bands: Initial results from Tampa Bay, FL. *Remote Sensing of Environment*, *93*(3), 423–441. https://doi.org/10.1016/j.rse.2004.08.007

Hu et al. - 2004—Assessment of estuarine water-quality indicators u.pdf. (n.d.).

Keith, D. J., Schaeffer, B. A., Lunetta, R. S., Gould, R. W., Rocha, K., & Cobb, D. J. (2014). Remote sensing of selected water-quality indicators with the hyperspectral imager for the coastal ocean (HICO) sensor. *International Journal of Remote Sensing*, *35*(9), 2927–2962. https://doi.org/10.1080/01431161.2014.894663

Kisi, O. (2013). Modeling of Dissolved Oxygen in River Water Using Artificial Intelligence Techniques. *Journal of Environmental Informatics*, 92–101. https://doi.org/10.3808/jei.201300248

Morel, A., & Prieur, L. (1977). Analysis of variations in ocean color1. *Limnology and Oceanography*, *22*(4), 709–722. https://doi.org/10.4319/lo.1977.22.4.0709

NASA Ocean Biology Processing Group. (2017). *MODIS-Aqua Level 2 Ocean Color Data Version R2018.0* [Data set]. NASA Ocean Biology DAAC. https://doi.org/10.5067/AQUA/MODIS/L2/OC/2018

NASA Ocean Color. (n.d.). Retrieved June 1, 2022, from https://oceancolor.gsfc.nasa.gov/data/aqua/

Nechad, B., Ruddick, K. G., & Neukermans, G. (2009). Calibration and validation of a generic multisensor algorithm for mapping of turbidity in coastal waters. *Remote Sensing of the Ocean, Sea Ice, and Large Water Regions 2009*, *7473*, 161–171. https://doi.org/10.1117/12.830700

Palani, S., Liong, S.-Y., & Tkalich, P. (2008). An ANN application for water quality forecasting. *Marine Pollution Bulletin*, *56*(9), 1586–1597. https://doi.org/10.1016/j.marpolbul.2008.05.021

Recknagel, F., French, M., Harkonen, P., & Yabunaka, K.-I. (1997). Artificial neural network approach for modelling and prediction of algal blooms. *Ecological Modelling*, *96*(1), 11–28. https://doi.org/10.1016/S0304-3800(96)00049-X

Ritchie, J., Spencer, L., & O'Connor, W. (2003). Carrying out qualitative analysis. *Qualitative Research Practice: A Guide for Social Science Students and Researchers*, *2003*, 219–262.

Rousso, B. Z., Bertone, E., Stewart, R., & Hamilton, D. P. (2020a). A systematic literature review of forecasting and predictive models for cyanobacteria blooms in freshwater lakes. *Water Research*, *182*, 115959. https://doi.org/10.1016/j.watres.2020.115959

Rousso, B. Z., Bertone, E., Stewart, R., & Hamilton, D. P. (2020b). A systematic literature review of forecasting and predictive models for cyanobacteria blooms in freshwater lakes. *Water Research*, *182*, 115959. https://doi.org/10.1016/j.watres.2020.115959

Salman, M. A., Fendereski, F., Hosseini, S. A., & Fazli, H. (2013). A MODIS-based estimation of chlorophyll a concentration using ANN model and in-situ measurements in the southern Caspian Sea..pdf. (n.d.).

Schaeffer, R., Szklo, A. S., Pereira de Lucena, A. F., Moreira Cesar Borba, B. S., Pupo Nogueira, L. P., Fleming, F. P., Troccoli, A., Harrison, M., & Boulahya, M. S. (2012). Energy sector vulnerability to climate change: A review. *Energy*, *38*(1), 1–12. https://doi.org/10.1016/j.energy.2011.11.056

SeaWiFS 项目—航天器和传感器概述. (n.d.). Retrieved June 1, 2022, from https://oceancolor.gsfc.nasa.gov/SeaWiFS/SEASTAR/SPACECRAFT.html

Topp, S. N., Pavelsky, T. M., Jensen, D., Simard, M., & Ross, M. R. V. (2020). Research Trends in the Use of Remote Sensing for Inland Water Quality Science: Moving Towards Multidisciplinary Applications. *Water*, *12*(1), 169. https://doi.org/10.3390/w12010169

Wang, F., Wang, X., Chen, B., Zhao, Y., & Yang, Z. (2013). Chlorophyll a Simulation in a Lake Ecosystem Using a Model with Wavelet Analysis and Artificial Neural Network. *Environmental Management*, *51*(5), 1044–1054. https://doi.org/10.1007/s00267-013-0029-5

Water Framework Directive. (n.d.). Retrieved June 27, 2022, from https://www.gov.ie/en/publication/f7c76-water-framework-directive/

Welcome to Waterinfo. (n.d.). Retrieved June 1, 2022, from https://www.waterinfo.be/

Werdell, P. J., McKinna, L. I. W., Boss, E., Ackleson, S. G., Craig, S. E., Gregg, W. W., Lee, Z., Maritorena, S., Roesler, C. S., Rousseaux, C. S., Stramski, D., Sullivan, J. M., Twardowski, M.

S., Tzortziou, M., & Zhang, X. (2018). An overview of approaches and challenges for retrieving marine inherent optical properties from ocean color remote sensing. *Progress in Oceanography*, *160*, 186–212. https://doi.org/10.1016/j.pocean.2018.01.001

Wilson, H., & Recknagel, F. (2001). Towards a generic artificial neural network model for dynamic predictions of algal abundance in freshwater lakes. *Ecological Modelling*, *146*(1), 69–84. https://doi.org/10.1016/S0304-3800(01)00297-6

Zhang, Q., & Stanley, S. J. (1997). Forecasting raw-water quality parameters for the North Saskatchewan River by neural network modeling. *Water Research*, *31*(9), 2340–2350. https://doi.org/10.1016/S0043-1354(97)00072-9